HEPATOLOGY
Official Journal of the American Association for the Study of Liver Diseases

Human Blood Dendritic Cell Antigen 3 (BDCA3)$^+$ Dendritic Cells Are a Potent Producer of Interferon-λ in Response to Hepatitis C Virus

Sachiyo Yoshio,[1] Tatsuya Kanto,[1] Shoko Kuroda,[1] Tokuhiro Matsubara,[1] Koyo Higashitani,[1] Naruyasu Kakita,[1] Hisashi Ishida,[1] Naoki Hiramatsu,[1] Hiroaki Nagano,[2] Masaya Sugiyama,[3] Kazumoto Murata,[3] Takasuke Fukuhara,[4] Yoshiharu Matsuura,[4] Norio Hayashi,[5] Masashi Mizokami,[3] and Tetsuo Takehara[1]

The polymorphisms in the interleukin (*IL)-28B* (interferon-lambda [IFN]-λ3) gene are strongly associated with the efficacy of hepatitis C virus (HCV) clearance. Dendritic cells (DCs) sense HCV and produce IFNs, thereby playing some cooperative roles with HCV-infected hepatocytes in the induction of interferon-stimulated genes (ISGs). Blood dendritic cell antigen 3 (BDCA3)$^+$ DCs were discovered as a producer of IFN-λ upon Toll-like receptor 3 (TLR3) stimulation. We thus aimed to clarify the roles of BDCA3$^+$ DCs in anti-HCV innate immunity. Seventy healthy subjects and 20 patients with liver tumors were enrolled. BDCA3$^+$ DCs, in comparison with plasmacytoid DCs and myeloid DCs, were stimulated with TLR agonists, cell-cultured HCV (HCVcc), or Huh7.5.1 cells transfected with HCV/JFH-1. BDCA3$^+$ DCs were treated with anti-CD81 antibody, inhibitors of endosome acidification, TIR-domain-containing adapter-inducing interferon-β (TRIF)-specific inhibitor, or ultraviolet-irradiated HCVcc. The amounts of IL-29/IFN-λ1, IL-28A/IFN-λ2, and IL-28B were quantified by subtype-specific enzyme-linked immunosorbent assay (ELISA). The frequency of BDCA3$^+$ DCs in peripheral blood mononuclear cell (PBMC) was extremely low but higher in the liver. BDCA3$^+$ DCs recovered from PBMC or the liver released large amounts of IFN-λs, when stimulated with HCVcc or HCV-transfected Huh7.5.1. BDCA3$^+$ DCs were able to induce ISGs in the coexisting JFH-1-positive Huh7.5.1 cells. The treatments of BDCA3$^+$ DCs with anti-CD81 antibody, cloroquine, or bafilomycin A1 reduced HCVcc-induced IL-28B release, whereas BDCA3$^+$ DCs comparably produced IL-28B upon replication-defective HCVcc. The TRIF-specific inhibitor reduced IL-28B release from HCVcc-stimulated BDCA3$^+$ DCs. In response to HCVcc or JFH-1-Huh7.5.1, BDCA3$^+$ DCs in healthy subjects with IL-28B major (rs8099917, TT) released more IL-28B than those with IL-28B minor genotype (TG). *Conclusion*: Human BDCA3$^+$ DCs, having a tendency to accumulate in the liver, recognize HCV in a CD81-, endosome-, and TRIF-dependent manner and produce substantial amounts of IL-28B/IFN-λ3, the ability of which is superior in subjects with IL-28B major genotype. (HEPATOLOGY 2013;57:1705-1715)

Hepatitis C virus (HCV) infection is one of the most serious health problems in the world. More than 170 million people are chronically infected with HCV and are at high risk of developing liver cirrhosis and hepatocellular carcinoma. Genome-wide association studies have successfully identified the genetic polymorphisms (single nucleotide polymorphisms, SNPs) upstream of the promoter region of the

Abbreviations: Ab, antibody; HCV, hepatitis C virus; HCVcc, cell-cultured hepatitis C virus; HSV, herpes simplex virus; IHL, intrahepatic lymphocyte; INF-λ, interferon-lambda; IRF, interferon regulatory factor; ISGs, interferon-stimulated genes; JEV, Japanese encephalitis virus; Lin, lineage; mDC, myeloid DC; MOI, multiplicity of infection; PBMC, peripheral blood mononuclear cell; pDC, plasmacytoid DC; Poly IC, polyinosine-polycytidylic acid; RIG-I, retinoic acid-inducible gene-I; SNPs, single nucleotide polymorphisms; TLR, Toll-like receptor; TRIF, TIR-domain-containing adapter-inducing interferon-β.

From the [1]Department of Gastroenterology and Hepatology, Osaka University Graduate School of Medicine, Osaka, Japan; [2]Department of Surgery, Osaka University Graduate School of Medicine, Osaka, Japan; [3]Research Center for Hepatitis and Immunology, National Center for Global Health and Medicine, Ichikawa, Japan; [4]Department of Molecular Virology, Research Institute for Microbial Diseases, Osaka University, Osaka, Japan; [5]Kansai Rosai Hospital, Hyogo, Japan.

Received July 2, 2012; accepted November 13, 2012.

Supported in part by a Grant-In-Aid for Scientific Research from the Ministry of Education, Culture, Sports, Science, and Technology, Japan and a Grant-In-Aid from the Ministry of Health, Labor, and Welfare of Japan.

interleukin (IL)-28B / interferon-lambda 3 (IFN-λ3) gene, which are strongly associated with the efficacy of pegylated interferon-α (PEG-IFN-α) and ribavirin therapy or spontaneous HCV clearance.[1-4]

IFN-λs, or type III IFNs, comprise a family of highly homologous molecules consisting of IFN-λ1 (IL-29), IFN-λ2 (IL-28A), and IFN-λ3 (IL-28B). In clear contrast to type I IFNs, they are released from relatively restricted types of cells, such as hepatocytes, intestinal epithelial cells, or dendritic cells (DCs). Also, the cells that express heterodimeric IFN-λ receptors (IFN-λR1 and IL-10R2) are restricted to cells of epithelial origin, hepatocytes, or DCs.[5] Such limited profiles of cells expressing IFN-λs and their receptors define the biological uniqueness of IFN-λs. It has been shown that IFN-λs convey anti-HCV activity by inducing various interferon-stimulated genes (ISGs),[5] the profiles of which were overlapped but others were distinct from those induced by IFN-α/β. Some investigators showed that the expression of IL-28 in PBMC was higher in subjects with IL-28B major than those with minor; however, the levels of IL-28 transcripts in liver tissue were comparable regardless of IL-28B genotype.[2,6]

At the primary exposure to hosts, HCV maintains high replicative levels in the infected liver, resulting in the induction of IFNs and ISGs. In a case of successful HCV eradication, it is postulated that IFN-α/β and IFN-λ cooperatively induce antiviral ISGs in HCV-infected hepatocytes. It is of particular interest that, in primary human hepatocytes or chimpanzee liver, IFN-λs, but not type I IFNs, are primarily induced after HCV inoculation, the degree of which is closely correlated with the levels of ISGs.[7] These results suggest that hepatic IFN-λ could be a principal driver of ISG induction in response to HCV infection. Nevertheless, the possibility remains that DCs, as a prominent IFN producer in the liver, play significant roles in inducing hepatic ISGs and thereby suppressing HCV replication.

DCs, as immune sentinels, sense specific genomic and/or structural components of pathogens with various pattern recognition receptors and eventually release IFNs and inflammatory cytokines.[8] In general, DCs migrate to the organ where inflammation or cellular apoptosis occurs and alter their function in order to alleviate or exacerbate the disease conditions. Therefore, the phenotypes and/or capacity of liver DCs are deemed to be influenced in the inflamed liver. In humans, the existence of phenotypically and functionally distinct DC subsets has been reported: myeloid DC (mDC) and plasmacytoid DC (pDC).[9] Myeloid DCs predominantly produce IL-12 or tumor necrosis factor alpha (TNF-α) following proinflammatory stimuli, while pDCs release considerable amounts of type I IFNs upon virus infection.[9] The other type of mDCs, mDC2 or BDCA3$^+$(CD141) DCs, have been drawing much attention recently, since human BDCA3$^+$ DCs are reported to be a counterpart of murine CD8a$^+$ DCs.[10] Of particular interest is the report that BDCA3$^+$ DCs have a potent capacity of releasing IFN-λ in response to Toll-like receptor 3 (TLR3) agonist.[11] However, it is still largely unknown whether human BDCA3$^+$ DCs are able to respond to HCV.

Taking these reports into consideration, we hypothesized that human BDCA3$^+$ DCs, as a producer of IFN-λs, have crucial roles in anti-HCV innate immunity. We thus tried to clarify the potential of BDCA3$^+$ DCs in producing type III IFNs by using cell-cultured HCV (HCVcc) or hepatoma cells harboring HCV as stimuli. Our findings show that BDCA3$^+$ DCs are quite a unique DC subset, characterized by a potent and specialized ability to secrete IFN-λs in response to HCV. The ability of BDCA3$^+$ DCs to release IL-28B upon HCV is superior in subjects with IL-28B major (rs8099917, TT) to those with minor (TG or GG) genotype, suggesting that BDCA3$^+$ DCs are one of the key players in IFN-λ-mediated innate immunity.

Patients and Methods

Subjects. This study enrolled 70 healthy volunteers (male/female: 61/9) (age: mean ± standard deviation [SD], 37.3 ± 7.8 years) and 20 patients who underwent surgical resection of liver tumors at Osaka University Hospital (Supporting Table 1). The study was approved by the Ethical Committee of Osaka University Graduate School of Medicine. Written informed consent was obtained from all of them. All healthy volunteers were negative for HCV, hepatitis B virus (HBV), and human immunodeficiency virus (HIV) and had no apparent history of liver, autoimmune, or malignant diseases.

Address reprint requests to: Tatsuya Kanto, M.D., Ph.D., Department of Gastroenterology and Hepatology, Osaka University Graduate School of Medicine, 2-2 Yamadaoka, Suita, 565-0871 Japan. E-mail: kantot@gh.med.osaka-u.ac.jp; fax: +81-6-6879-3629.

View this article online at wileyonlinelibrary.com.

DOI 10.1002/hep.26182

Potential conflict of interest: Nothing to report.

Additional Supporting Information may be found in the online version of this article.

Reagents. The specifications of all antibodies used for FACS or cell sorting TLR-specific synthetic agonists, pharmacological reagents, and inhibitory peptides are listed in the Supporting Materials.

Separation of DCs from PBMC or Intrahepatic Lymphocytes. We collected 400 mL of blood from each healthy volunteer and processed them for PBMCs. Noncancerous liver tissues were obtained from patients who underwent resection of liver tumors (Supporting Table 1). For the collection of intrahepatic lymphocytes (IHLs), liver tissues were washed thoroughly with phosphate-buffered saline to remove the peripheral blood adhering to the tissue and ground gently. After Lin-negative ($CD3^-$, $CD14^-$, $CD19^-$, and $CD56^-$) cells were obtained by the MACS system, each DC subset with the defined phenotype was sorted separately under FACS Aria (BD). The purity was more than 98%, as assessed by FACS Canto II (BD). Sorted DCs were cultured at 2.5×10^4/well on 96-well culture plates.

Immunofluorescence Staining of Human Liver Tissue. Tissue specimens were obtained from surgical resections of noncancerous liver from the patients as described above. Briefly, the 5-mm sections were incubated with the following antibodies: mouse biotinylated antihuman BDCA3 antibody (Miltenyi-Biotec), and mouse antihuman CLEC9A antibody (Biolegend) and subsequently with secondary goat antirabbit Alexa Fluor488 or goat antimouse Alexa Fluor594 (Invitrogen, Molecular Probes) antibodies. Cell nuclei were counterstained with Dapi-Fluoromount-GTM (Southern Biotech, Birmingham, AL). The stained tissues were analyzed by fluorescence microscopy (Model BZ-9000; Keyence, Osaka, Japan).

Cells and Viruses. The *in vitro* transcribed RNA of the JFH-1 strain of HCV was introduced into FT3-7 cells[12] or Huh7.5.1 cells. The stocks of HCVcc were generated by concentration of the medium from JFH-1-infected FT3-7 cells. The virus titers were determined by focus forming assay.[13] The control medium was generated by concentration of the medium from HCV-uninfected FT3-7 cells. Infectious JEVs were generated from the expression plasmid (pMWJEATG1) as reported.[14] HSV (KOS) was a generous gift from Dr. K. Ueda (Osaka University). Huh7.5.1 cells transduced with HCV JFH-1 strain was used for the coculture with DCs. The transcripts of ISGs in Huh7.5.1 were examined by reverse-transcription polymerase chain reaction (RT-PCR) methods using gene-specific primers and probes (Applied Biosystems, Foster City, CA).

Secretion Assays. IL-28B/IFN-λ3 was quantified by a newly developed chemiluminescence enzyme immunoassay (CLEIA) system.[15] IL-29/IFN-λ1, IL-28A/IFN-λ2, and IFN-β were assayed by commercially available enzyme-linked immunosorbent assay (ELISA) kits (eBioscience, R&D, and PBL, respectively). IFN-α was measured by cytometric beads array kits (BD) according to the manufacturer's instructions.

Statistical Analysis. The differences between two groups were assessed by the Mann-Whitney nonparametric *U* test. Multiple comparisons between more than two groups were analyzed by the Kruskal-Wallis nonparametric test. Paired *t* tests were used to compare differences in paired samples. All the analyses were performed using GraphPad Prism software (San Diego, CA).

Results

Human BDCA3$^+$ DCs Are Phenotypically Distinct from pDCs and mDCs. We defined BDCA3$^+$ DCs as $Lin^-HLA\text{-}DR^+BDCA3^{high+}$ cells (Fig. 1A, left, middle), and pDCs and mDCs by the patterns of CD11c and CD123 expressions (Fig. 1A, right). The level of CD86 on pDCs or mDCs is comparatively higher than those on BDCA3$^+$ DCs (Fig. 1B). The expression of CD81 is higher on BDCA3$^+$ DCs than on pDCs and mDCs (Fig. 1B, Supporting Fig. S1). CLEC9A, a member of C-type lectin, is expressed specifically on BDCA3$^+$ DCs as reported elsewhere,[16] but not on pDCs and mDCs (Fig. 1B).

Liver BDCA3$^+$ DCs Are More Mature than the Counterparts in the Periphery. BDCA3$^+$ DCs in infiltrated hepatic lymphocytes (IHLs) are all positive for CLEC9A, but liver pDCs or mDCs are not (data not shown). The levels of CD40, CD80, CD83, and CD86 on liver BDCA3$^+$ DCs are higher than those on the peripheral counterparts, suggesting that BDCA3$^+$ DCs are more mature in the liver compared to those in the periphery (Fig. 1C).

In order to confirm that BDCA3$^+$ DCs are localized in the liver, we stained the cells with immunofluorescence antibodies (Abs) in noncancerous liver tissues. Liver BDCA3$^+$ DCs were defined as BDCA3$^+$ CLEC9A$^+$ cells (Fig. 1D). Most of the cells were found near the vascular compartment or in sinusoid or the space of Disse of the liver tissue.

BDCA3$^+$ DCs Are Scarce in PBMCs but More Abundant in the Liver. The percentages of BDCA3$^+$ DCs in PBMCs were much lower than those of the other DC subsets (BDCA3$^+$ DCs, pDCs and mDCs, mean $\pm$ SD [%], 0.054 ± 0.044, 0.27 ± 0.21 and 1.30 ± 0.65) (Fig. 2A). The percentages of BDCA3$^+$ DCs in IHLs were lower than those of the others (BDCA3$^+$ DCs, pDCs, and mDCs, mean $\pm$ SD [%],

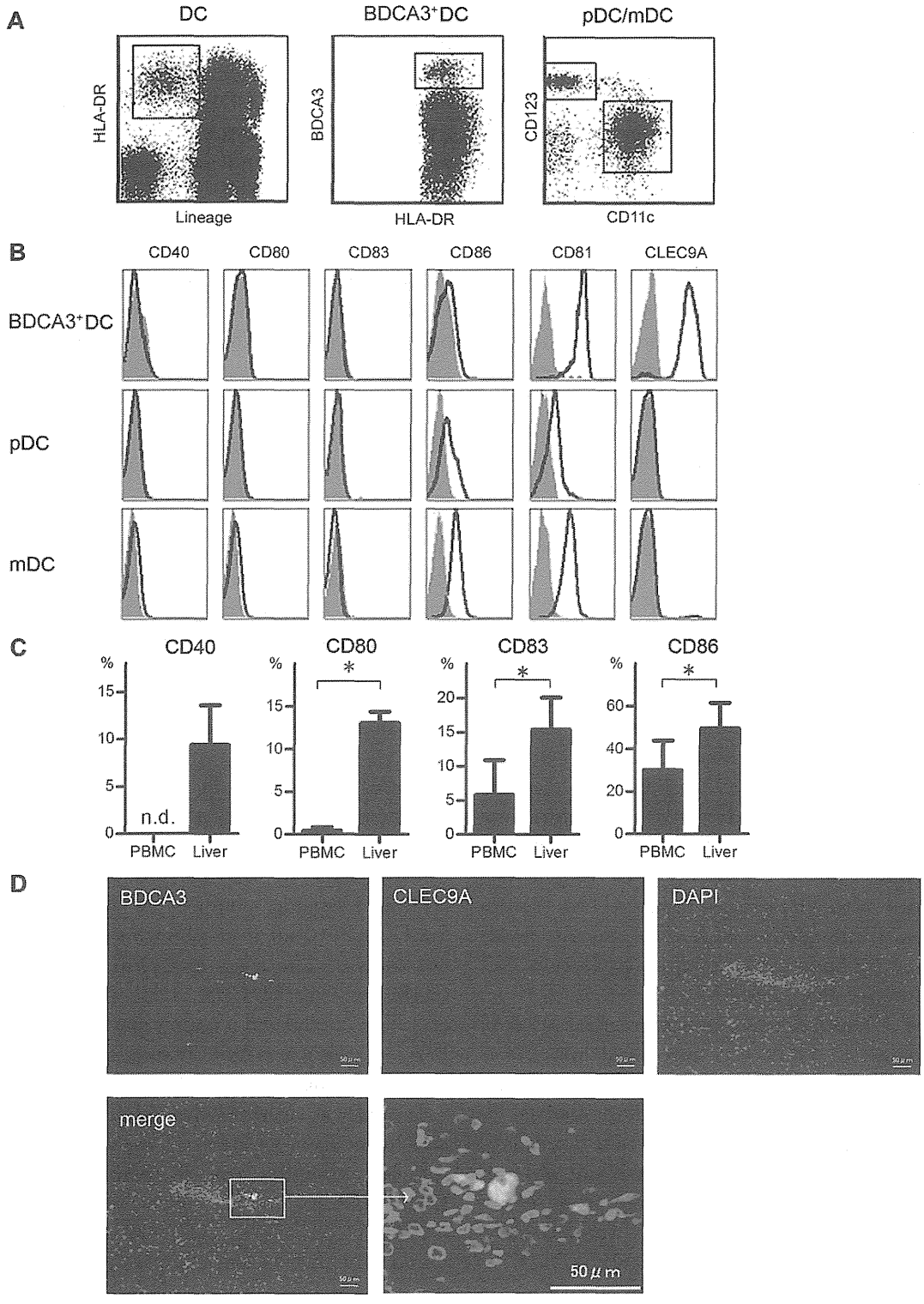

Fig. 1. Identification and phenotypic analyses of peripheral blood and intrahepatic BDCA3^{+} DCs. (A) We defined BDCA3^{+} DCs as Lineage^{-}HLA-DR^{+}BDCA3^{high+} cells (middle), pDCs as Lineage^{-}HLA-DR^{+}CD11c^{-}CD123^{high+} cells, and mDCs as Lineage^{-}HLA-DR^{+}CD11c^{+}CD123^{low+} cells (right). (B) The expressions of CD40, CD80, CD83, CD86, CD81, and CLEC9A on each DC subset in peripheral blood are shown. Representative results of five donors are shown in the histograms. Filled gray histograms depict data with isotype Abs, and open black ones are those with specific Abs. (C) The expressions of costimulatory molecules on BDCA3^{+} DCs were compared between in PBMCs and in the liver. The results are shown as the percentage of positive cells. Results are the mean ± SEM from four independent experiments. *$P < 0.05$ by paired t test. (D) The staining for BDCA3 (green), CLEC9A (red) identifies BDCA3^{+} DCs (merge, BDCA3^{+}CLEC9A^{+}) in human liver tissues. Representative results of the noncancerous liver samples are shown. BDCA, blood dendritic cell antigen; pDC, plasmacytoid DC; mDC, myeloid DC; CLEC9A, C-type lectin 9A.

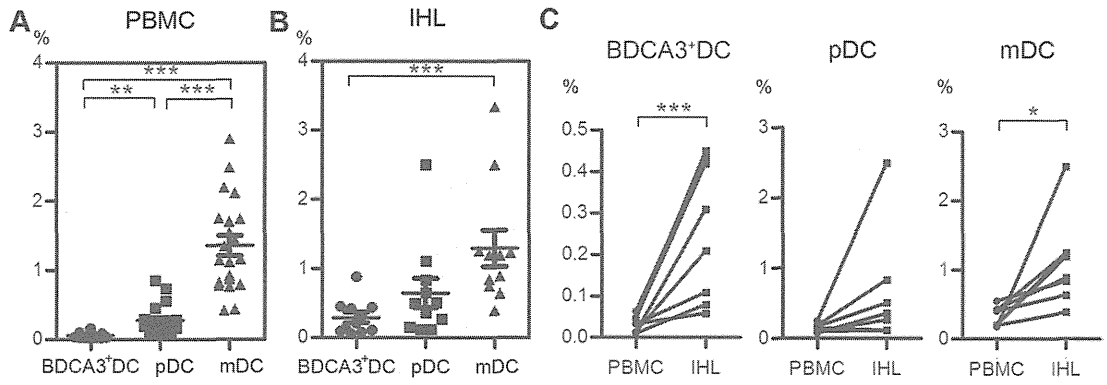

Fig. 2. Analysis of frequency of DC subsets in the peripheral blood and in the liver. Frequencies of BDCA3$^+$ DCs, pDCs, and mDCs in PBMCs (21 healthy subjects) (A) or in the intrahepatic lymphocytes (IHLs) (11 patients who had undergone surgical resection of tumors) (B) are shown. Horizontal bars depict the mean ± SD. $^{**}P < 0.005$; $^{***}P < 0.0005$ by Kruskal-Wallis test. (C) The paired comparisons of the frequencies of DC subsets between in PBMCs and in IHLs. the results of eight patients whose PBMCs and IHLs were obtained simultaneously are shown. $^{*}P < 0.05$; $^{***}P < 0.0005$ by paired *t* test. IHLs, intrahepatic lymphocytes; pDC and mDC, see Fig. 1.

0.29 ± 0.25, 0.65 ± 0.69 and 1.2 ± 0.94) (Fig. 2B). The percentages of BDCA3$^+$ DCs in the IHLs were significantly higher than those in PBMCs from relevant donors (Fig. 2C). Such relative abundance of BDCA3$^+$ DCs in the liver over that in the periphery was observed regardless of the etiology of the liver disease (Supporting Table 1).

BDCA3$^+$ DCs Produce a Large Amount of IFN-λs upon Poly IC Stimulation. We compared DC subsets for their abilities to produce IL-29/IFN-λ1, IL-28A/IFN-λ2, IL-28B/IFN-λ3, IFN-β, and IFN-α in response to TLR agonists. Approximately 4.0×10^4 of BDCA3$^+$ DCs were recoverable from 400 mL of donated blood from healthy volunteers. We fixed the number of DCs at 2.5×10^4 cells/100 mL for comparison in the following experiments.

BDCA3$^+$ DCs have been reported to express mRNA for TLR1, 2, 3, 6, 8, and 10.[17] First, we quantified IL-28B/IFN-λ3 as a representative for IFN-λs after stimulation of BDCA3$^+$ DCs with relevant TLR agonists. We confirmed that BDCA3$^+$ DCs released IL-28B robustly in response to TLR3 agonist/poly IC but not to other TLR agonists (Fig. S2). In contrast, pDCs produced IL-28B in response to TLR9 agonist/CpG but much lesser to other agonists (Fig. S2). Next, we compared the capabilities of DCs inducing IFN-λs and IFN-β genes in response to relevant TLR agonists. BDCA3$^+$ DCs expressed extremely high levels of IL-29, IL-28A, and IL-28B transcripts compared to other DCs, whereas pDCs induced a higher level of IFN-β than other DCs (Fig. S3A).

Similar results were obtained with the protein levels of IFN-λs, IFN-β, and IFN-α released from DC subsets stimulated with TLR agonists. BDCA3$^+$ DCs produce significantly higher levels of IL-29, IL-28B, and IL-28A than the other DC subsets. In clear contrast, pDCs release a significantly larger amount of IFN-β and IFN-α than BDCA3$^+$ DCs or mDCs (Fig. 3A, Fig. S3B). As for the relationship among the quantity of IFN-λ subtypes from poly IC-stimulated BDCA3$^+$ DCs, the levels of IL-29/IFN-λ1 and IL-28B/IFN-λ3 were positively correlated ($R^2 = 0.76$, $P < 0.05$), and those of IL-28A/IFN-λ2 and IL-28B/IFN-λ3 were positively correlated as well ($R^2 = 0.84$, $P < 0.0005$), respectively (Fig. S3C). These results show that the transcription and translation machineries of IFN-λs may be overlapped among IFN-λ subtypes in BDCA3$^+$ DCs upon poly IC stimulation.

Liver BDCA3$^+$ DCs sorted from IHLs possess the ability to produce IL-28B in response to poly IC (Fig. 3B), showing that they are comparably functional. In response to poly IC, BDCA3$^+$ DCs were capable of producing inflammatory cytokines as well, such as TNF-α, IL-6, and IL-12p70 (Fig. S4A). By using Huh7 cells harboring HCV subgenomic replicons (HCV-N, genotype 1b), we confirmed that the supernatants from poly IC-stimulated BDCA3$^+$ DCs suppressed HCV replication in an IL-28B concentration-dependent manner (Fig. S4B). Therefore, poly IC-stimulated BDCA3$^+$ DCs are capable of producing biologically active substances suppressing HCV replication, some part of which may be mediated by IFN-λs.

BDCA3$^+$ DCs Produce IL-28B upon HCVcc or HCV/JFH-1-Transfected Huh7.5.1 Cells. We stimulated freshly isolated BDCA3$^+$ DCs, pDCs and mDCs with infectious viruses, such as HCVcc, Japanese encephalitis virus (JEV), and herpes simplex virus (HSV). In preliminary experiments, we confirmed that HCVcc stimulated BDCA3$^+$ DCs to release IL-28B in a dose-dependent manner (Fig. S5). BDCA3$^+$ DCs

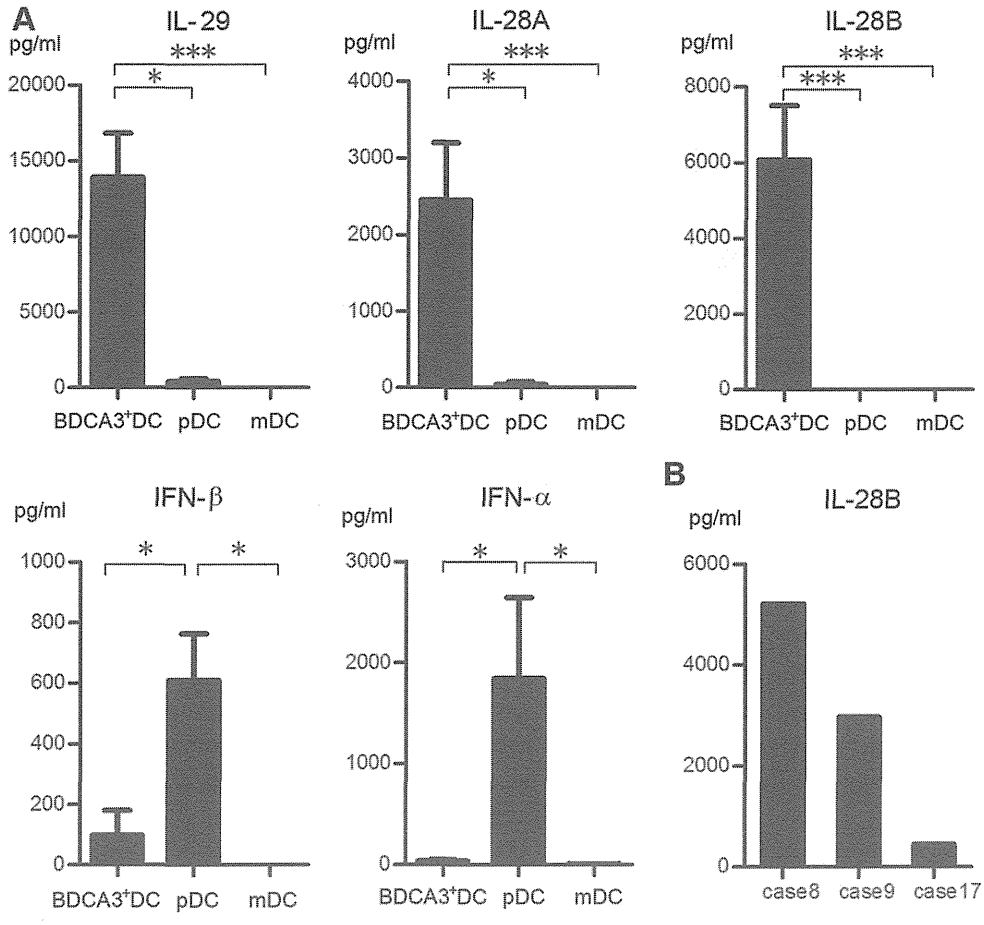

Fig. 3. BDCA3$^+$ DCs recovered from peripheral blood or intrahepatic lymphocytes produce large amounts of IL-29/IFN-λ1, IL-28A/IFN-λ2, and IL-28B/IFN-λ3 in response to poly IC. (A) BDCA3$^+$ DCs and mDCs were cultured at 2.5×10^4 cells with 25 mg/mL poly IC, and pDCs were with 5 mM CPG for 24 hours. The supernatants were examined for IL-29, IL-28A, IL-28B, IFN-β and IFN-α. Results are shown as mean $\pm$ SEM from 15 experiments. $^*P < 0.05$; $^{***}P < 0.0005$ by Kruskal-Wallis test. (B) For the IL-28B production, BDCA3$^+$ DCs in intrahepatic lymphocytes were cultured at 2.5×10^4 cells with 25 mg/mL poly IC for 24 hours. The samples of cases 8 and 9 were obtained from patients with non-B, non-C liver disease and that of case 17 was from an HCV-infected patient (Supporting Table 1).

produced a large amount of IL-28B upon exposure to HCVcc and released a lower amount of IFN-α upon HCVcc or HSV (Fig. 4A). In contrast, pDCs produced a large amount of IFN-α in response to HCVcc and HSV and a much lower level of IL-28B upon HCVcc (Fig. S6). In mDCs, IL-28B and IFN-α were not detectable with any of these viruses (data not shown).

BDCA3$^+$ DCs produced significantly higher levels of IL-28B than the other DCs upon HCVcc stimulation (Fig. 4B). By contrast, HCVcc-stimulated pDCs released significantly larger amounts of IFN-β and IFN-α than the other subsets (Fig. 4B). Liver BDCA3$^+$ DCs were capable of producing IL-28B in response to HCVcc (Fig. 4C). These results show that, upon HCVcc stimulation, BDCA3$^+$ DCs produce more IFN-λs and pDCs release more IFN-β and IFN-α than the other DC subsets, respectively. Taking a clinical impact of IL-28B genotypes on HCV eradication into consideration, we focused on IL-28B/IFN-λ3 as a representative for IFN-λs in the following experiments.

In a coculture with JFH-1-infected Huh7.5.1 cells, BDCA3$^+$ DCs profoundly released IL-29, IL-28A, and IL-28B (Fig. 4D, the results of IL-29 and IL-28A, not shown), whereas BDCA3$^+$ DCs failed to respond to Huh7.5.1 cells lacking HCV/JFH-1, showing that IL-28B production from BDCA3$^+$ DCs is dependent on HCV genome (Fig. 4D). In the absence of BDCA3$^+$ DCs, IL-28B is undetectable in the supernatant from JFH-1-infected Huh7.5.1 cells, demonstrating that BDCA3$^+$ DCs, not HCV-replicating Huh7.5.1 cells, produce detectable amount of IL-28B (Fig. 4D). In the coculture, BDCA3$^+$ DCs comparably released IL-28B either in the presence or the absence of transwells, suggesting that cell-to-cell contact between DCs and Huh7.5.1 cells is dispensable for IL-28B response (Fig. 4E). In parallel with the quantity of IL-28B in the coculture, ISG15 was significantly induced only in JFH-1-infected Huh7.5.1 cells cocultured with BDCA3$^+$ DCs (Fig. 4F). A strong induction was observed with other ISGs in JFH-1-infected Huh7.5.1 in the presence of BDCA3$^+$ DCs, such as IFIT1, MxA, RSD2, IP-10, and USP18 (Fig. S7). The results clearly show that BDCA3$^+$ DCs are capable of producing large amounts of IFN-λs in response to cellular or cell-free HCV, thereby inducing various ISGs in bystander liver cells.

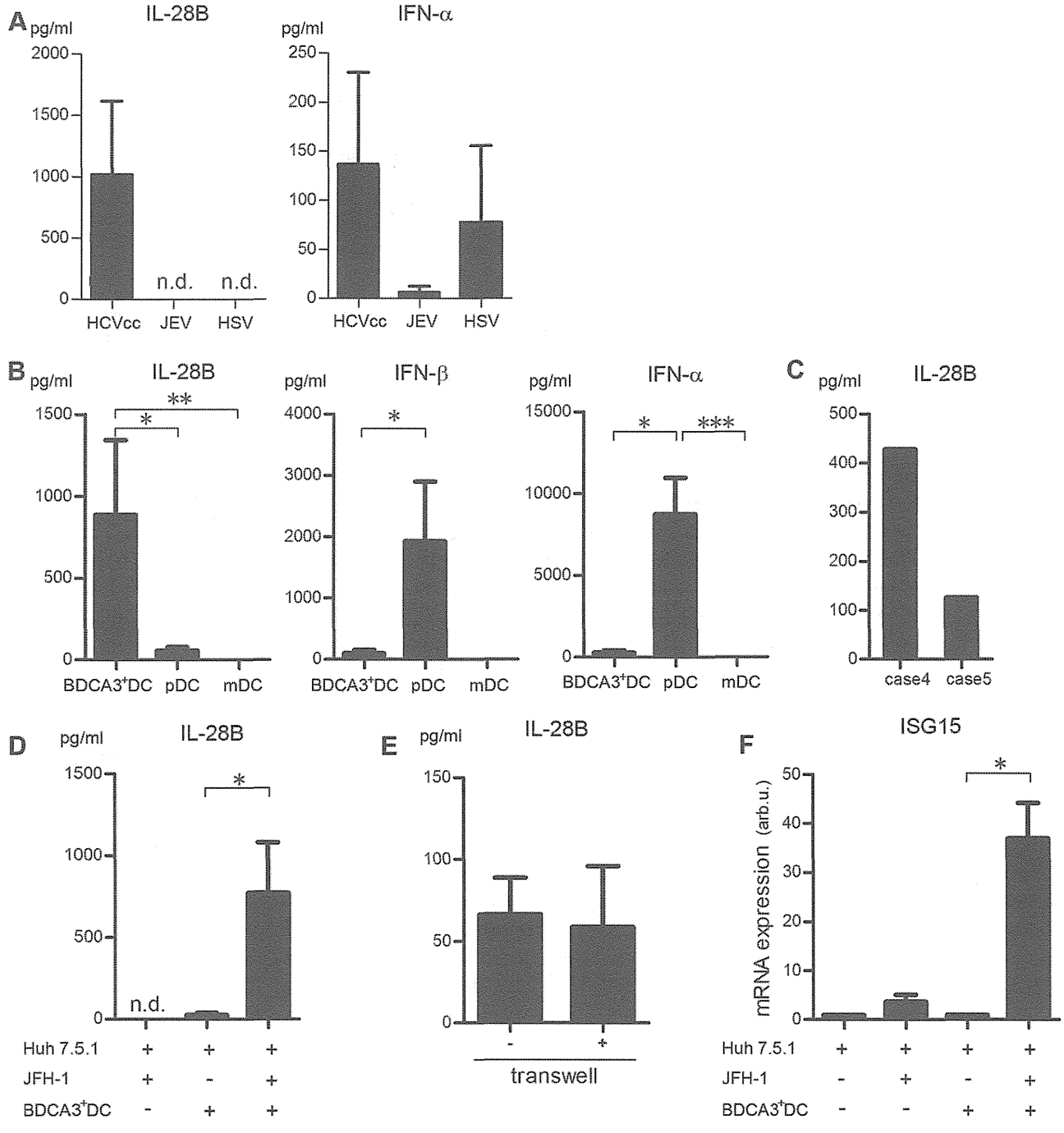

Fig. 4. BDCA3$^+$ DCs produce IL-29, IL-28A, and IL-28B upon cell-cultured HCV or HCV/JFH-1-transfected Huh7.5.1 cells, thereby inducing ISG. (A) BDCA3$^+$ DCs were cultured at 2.5 $\times$ 10^4 cells for 24 hours with HCVcc, JEV, or HSV at a multiplicity of infection (MOI) of 10. Results are shown as mean $\pm$ SEM from six experiments. n.d.; not detected. (B) BDCA3$^+$ DCs, pDCs, and mDCs were cultured at 2.5 $\times$ 10^4 cells for 24 hours with HCVcc at an MOI of 10. The results are shown as mean $\pm$ SEM from 11 experiments. *$P < 0.05$; **$P < 0.0005$; ***$P < 0.0005$ by Kruskal-Wallis test. (C) BDCA3$^+$ DCs recovered from intrahepatic lymphocytes were cultured at 2.5 $\times$ 10^4 cells for 24 hours with HCVcc at an MOI of 10. Both of the samples (cases 4 and 5) were obtained from patients with non-B, non-C liver disease. (D,E) BDCA3$^+$ DCs were cocultured at 2.5 $\times$ 10^4 cells with JFH-1-transfected (MOI = 2) or -untransfected Huh7.5.1 cells for 24 hours. The supernatants of JFH-1-transfected Huh7.5.1.cells without BDCA3$^+$ DCs were also examined. In some experiments of the coculture with JFH-1-transfected Huh7.5.1 cells and BDCA3$^+$ DCs, transwells were inserted into the wells (E). Results are shown as mean $\pm$ SEM from five experiments. *$P < 0.05$ by paired t test. (F) BDCA3$^+$ DCs were cocultured at 2.5 $\times$ 10^4 cells with JFH-1-transfected Huh7.5.1 cells (MOI = 2) or -untransfected Huh7.5.1 cells for 24 hours. The Huh7.5.1.cells were harvested and subjected to real-time RT-PCR analyses for ISG15 expression. The results are shown as mean $\pm$ SEM from five experiments. *$P < 0.05$ by paired t test. HCVcc, cell-cultured HCV; JEV, Japanese encephalitis virus; HSV, herpes simplex virus.

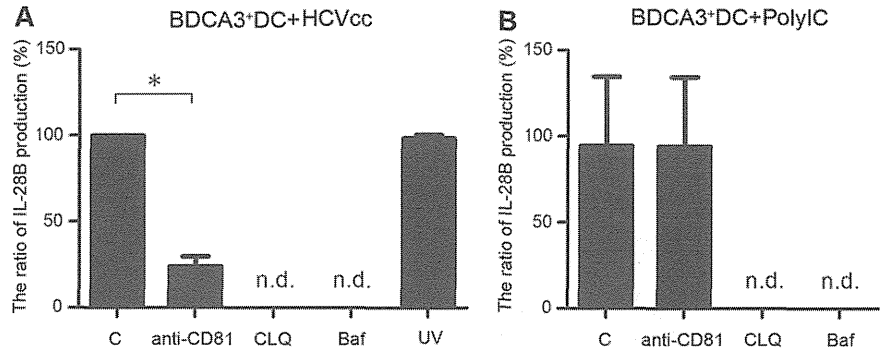

Fig. 5. The CD81 and endosome acidification is involved in the production of IL-28B from HCV-stimulated BDCA3$^+$ DCs, but HCV replication is not necessary. (A,B) BDCA3$^+$ DCs were cultured at 2.5 $\times$ 10^4 cells with HCVcc at an MOI of 10 (A) or poly IC (25 μg/mL) (B). In some experiments, UV-irradiated HCVcc was used at the same MOI, and BDCA3$^+$ DCs were treated with anti-CD81Ab (5 mg/mL), chloroquine (10 mM), or bafilomycin A1 (25 nM). The results are expressed as ratios of IL-28B quantity with or without the treatments. They are shown as mean $\pm$ SEM from five experiments. *$P < 0.05$ by paired t test. C, control; CLQ, treatment with chloroquine; Baf, treatment with bafilomycin A1; UV, ultraviolet-irradiated HCVcc; n.d., not detected.

CD81 and Endosome Acidification Are Involved in IL-28B Production from HCV-Stimulated BDCA3$^+$ DCs, but HCV Replication Is Not Involved. It is not known whether HCV entry and subsequent replication in DCs is involved or not in IFN response.[18,19] To test this, BDCA3$^+$ DCs were inoculated with UV-irradiated, replication-defective HCVcc. We confirmed that UV exposure under the current conditions is sufficient to negate HCVcc replication in Huh7.5.1 cells, as demonstrated by the lack of expression of NS5A after inoculation (data not shown). BDCA3$^+$ DCs produced comparable levels of IL-28B with UV-treated HCVcc, indicating that active HCV replication is not necessary for IL-28B production (Fig. 5A).

We next examined whether or not the association of HCVcc with BDCA3$^+$ DCs by CD81 is required for IL-28B production. It has been reported that the E2 region of HCV structural protein is associated with CD81 on cells when HCV enters susceptible cells.[13,20] We confirmed that all DC subsets express CD81, the degree of which was most significant on BDCA3$^+$ DCs (Fig. 1B, Fig. S1). Masking of CD81 with Ab significantly impaired IL-28B production from HCVcc-stimulated BDCA3$^+$ DCs in a dose-dependent manner (Fig. 5A, Fig. S8), suggesting that HCV-E2 and CD81 interaction is involved in the induction. The treatment of poly IC-stimulated BDCA3$^+$ DCs with anti-CD81 Ab failed to suppress IL-28B production (Fig. 5B).

HCV enters the target cells, which is followed by fusion steps within acidic endosome compartments. Chloroquine and bafilomycin A1 are well-known and broadly used inhibitors of endosome TLRs, which are reported to be capable of blocking TLR3 response in human monocyte-derived DC.[21,22] In our study, the treatment of BDCA3$^+$ DCs with chloroquine, bafilomycin A1, or NH4Cl significantly suppressed their IL-28B production either in response to HCVcc or poly IC (Fig. 5A,B, NH4Cl, data not shown). These results suggest that the endosome acidification is involved in HCVcc- or poly IC-stimulated BDCA3$^+$ DCs to produce IL-28B. The similar results were obtained with HCVcc-stimulated pDCs for the production of IL-28B (Fig. S9). We validated that such concentration of chloroquine (10 mM) and bafilomycin A1 (25 nM) did not reduce the viability of BDCA3$^+$ DCs (Fig. S10).

BDCA3$^+$ DCs Produce IL-28B in Response to HCVcc by a TIR-Domain-Containing Adapter-Inducing Interferon-β (TRIF)-Dependent Mechanism. TRIF/TICAM-1, a TIR domain-containing adaptor, is known to be essential for the TLR3-mediated pathway.[23] In order to elucidate whether TLR3-dependent pathway is involved or not in IL-28B response of BDCA3$^+$ DCs, we added the cell-permeable TRIF-specific inhibitory peptide (Invivogen) or the control peptide to poly IC- or HCVcc-stimulated BDCA3$^+$ DCs. Of particular interest, the TRIF-specific inhibitor peptide, but not the control one, significantly suppressed IL-28B production from poly IC- or HCVcc-stimulated BDCA3$^+$ DCs (Fig. 6A,B). In clear contrast, the TRIF-specific inhibitor failed to suppress IL-28B from HCVcc-stimulated pDCs (Fig. 6C), suggesting that pDCs recognize HCVcc in an endosome-dependent but TRIF-independent pathway. These results show that BDCA3$^+$ DCs may recognize HCVcc by way of the TRIF-dependent pathway to produce IL-28B.

BDCA3$^+$ DCs in Subjects with IL-28B Major Genotype Produce More IL-28B in Response to HCV than Those with IL-28B Minor Type. In order to compare the ability of BDCA3$^+$ DCs to release IL-28B in healthy subjects between IL28B major (rs8099917, TT)

involved in IL-28B gene according to the IL-28B genotypes. Recently, in influenza virus infection, it is reported that micro-RNA29 and DNA methyltransferase are involved in the cyclooxygenase-2-mediated enhancement of IL-29/IFN-λ1 production.[27] This report supports the possibility that similar epigenetic machineries could be operated as well in HCV-induced IFN-λs production. Second, it is plausible that the efficiency of the stimulation of TLR3-TRIF may be different between the IL-28B genotypes. Since HCV reaches endosome in BDCA3$^+$ DCs by way of the CD81-mediated entry and subsequent endocytosis pathways, the efficiencies of HCV handling and enzyme reactions in endosome may be influential in the subsequent TLR3-TRIF-dependent responses. Certain unknown factors regulating such process may be linked to the IL-28B genotypes. For a comprehensive understanding of the biological importance of IL-28B in HCV infection, such confounding factors, if they exist, need to be explored.

In conclusion, human BDCA3$^+$ DCs, having a tendency to accumulate in the liver, recognize HCV and produce large amounts of IFN-λs. An enhanced IL-28B/IFN-λ3 response of BDCA3$^+$ DCs to HCV in subjects with IL-28B major genotype suggests that BDCA3$^+$ DCs are one of the key players in anti-HCV innate immunity. An exploration of the molecular mechanisms of potent and specialized capacity of BDCA3$^+$ DCs as IFN-λ producer could provide useful information on the development of a natural adjuvant against HCV infection.

References

1. Suppiah V, Moldovan M, Ahlenstiel G, Berg T, Weltman M, Abate ML, et al. IL28B is associated with response to chronic hepatitis C interferon-alpha and ribavirin therapy. Nat Genet 2009;41:1100-1104.
2. Tanaka Y, Nishida N, Sugiyama M, Kurosaki M, Matsuura K, Sakamoto N, et al. Genome-wide association of IL28B with response to pegylated interferon-alpha and ribavirin therapy for chronic hepatitis C. Nat Genet 2009;41:1105-1109.
3. Ge D, Fellay J, Thompson AJ, Simon JS, Shianna KV, Urban TJ, et al. Genetic variation in IL28B predicts hepatitis C treatment-induced viral clearance. Nature 2009;461:399-401.
4. Thomas DL, Thio CL, Martin MP, Qi Y, Ge D, O'Huigin C, et al. Genetic variation in IL28B and spontaneous clearance of hepatitis C virus. Nature 2009;461:798-801.
5. Kotenko SV. IFN-lambdas. Curr Opin Immunol 2011;23:583-590.
6. Urban TJ, Thompson AJ, Bradrick SS, Fellay J, Schuppan D, Cronin KD, et al. IL28B genotype is associated with differential expression of intrahepatic interferon-stimulated genes in patients with chronic hepatitis C. Hepatology 2010;52:1888-1896.
7. Park H, Serti E, Eke O, Muchmore B, Prokunina-Olsson L, Capone S, et al. IL-29 is the dominant type III interferon produced by hepatocytes during acute hepatitis C virus infection. Hepatology 2012;56:2060-2070.
8. Medzhitov R. Recognition of microorganisms and activation of the immune response. Nature 2007;449:819-826.
9. Liu YJ. Dendritic cell subsets and lineages, and their functions in innate and adaptive immunity. Cell 2001;106:259-262.
10. Poulin LF, Salio M, Griessinger E, Anjos-Afonso F, Craciun L, Chen JL, et al. Characterization of human DNGR-1+ BDCA3+ leukocytes as putative equivalents of mouse CD8alpha+ dendritic cells. J Exp Med 2010;207:1261-1271.
11. Lauterbach H, Bathke B, Gilles S, Traidl-Hoffmann C, Luber CA, Fejer G, et al. Mouse CD8alpha+ DCs and human BDCA3+ DCs are major producers of IFN-lambda in response to poly IC. J Exp Med 2010;207:2703-2717.
12. Wakita T, Pietschmann T, Kato T, Date T, Miyamoto M, Zhao Z, et al. Production of infectious hepatitis C virus in tissue culture from a cloned viral genome. Nat Med 2005;11:791-796.
13. Lindenbach BD, Evans MJ, Syder AJ, Wolk B, Tellinghuisen TL, Liu CC, et al. Complete replication of hepatitis C virus in cell culture. Science 2005;309:623-626.
14. Mori Y, Okabayashi T, Yamashita T, Zhao Z, Wakita T, Yasui K, et al. Nuclear localization of Japanese encephalitis virus core protein enhances viral replication. J Virol 2005;79:3448-3458.
15. Sugiyama M, Kimura T, Naito S, Mukaide M, Shinauchi T, Ueno M, et al. Development of interferon lambda 3 specific quantification assay for its mRNA and serum/plasma specimens. Hepatol Res 2012;42:1089-1099.
16. Schreibelt G, Klinkenberg LJ, Cruz LJ, Tacken PJ, Tel J, Kreutz M, et al. The C type lectin receptor CLEC9A mediates antigen uptake and (cross-)presentation by human blood BDCA3+ myeloid dendritic cells. Blood 2012;119:2284-2292.
17. Jongbloed SL, Kassianos AJ, McDonald KJ, Clark GJ, Ju X, Angel CE, et al. Human CD141+ (BDCA-3)+ dendritic cells (DCs) represent a unique myeloid DC subset that cross-presents necrotic cell antigens. J Exp Med 2010;207:1247-1260.
18. Marukian S, Jones CT, Andrus L, Evans MJ, Ritola KD, Charles ED, et al. Cell culture-produced hepatitis C virus does not infect peripheral blood mononuclear cells. Hepatology 2008;48:1843-1850.
19. Liang H, Russell RS, Yonkers NL, McDonald D, Rodriguez B, Harding CV, et al. Differential effects of hepatitis C virus JFH1 on human myeloid and plasmacytoid dendritic cells. J Virol 2009;83:5693-5707.
20. Zhang J, Randall G, Higginbottom A, Monk P, Rice CM, McKeating JA. CD81 is required for hepatitis C virus glycoprotein-mediated viral infection. J Virol 2004;78:1448-1455.
21. Blanchard E, Belouzard S, Goueslain L, Wakita T, Dubuisson J, Wychowski C, et al. Hepatitis C virus entry depends on clathrin-mediated endocytosis. J Virol 2006;80:6964-6972.
22. de Bouteiller O, Merck E, Hasan UA, Hubac S, Benguigui B, Trinchieri G, et al. Recognition of double-stranded RNA by human toll-like receptor 3 and downstream receptor signaling requires multimerization and an acidic pH. J Biol Chem 2005;280:38133-38145.
23. Takeda K, Akira S. TLR signaling pathways. Semin Immunol 2004;16:3-9.
24. Velazquez VM, Hon H, Ibegbu C, Knechtle SJ, Kirk AD, Grakoui A. Hepatic enrichment and activation of myeloid dendritic cells during chronic hepatitis C virus infection. Hepatology 2012;56:2071-2081.
25. Dental C, Florentin J, Aouar B, Gondois-Rey F, Durantel D, Baumert TF, et al. Hepatitis C virus fails to activate NF-kappaB signaling in plasmacytoid dendritic cells. J Virol 2012;86:1090-1096.
26. Thomas E, Gonzalez VD, Li Q, Modi AA, Chen W, Noureddin M, et al. HCV infection induces a unique hepatic innate immune response associated with robust production of type III interferons. Gastroenterology 2012;142:978-988.
27. Fang J, Hao Q, Liu L, Li Y, Wu J, Huo X, Zhu Y. Epigenetic changes mediated by microRNA miR29 activate cyclooxygenase 2 and lambda-1 interferon production during viral infection. J Virol 2012;86:1010-1020.

JVI
Journals.ASM.org

Ifit1 Inhibits Japanese Encephalitis Virus Replication through Binding to 5′ Capped 2′-O Unmethylated RNA

Taishi Kimura,[a,b] Hiroshi Katoh,[d] Hisako Kayama,[a,b,f] Hiroyuki Saiga,[a] Megumi Okuyama,[a] Toru Okamoto,[d] Eiji Umemoto,[a,b,f] Yoshiharu Matsuura,[d] Masahiro Yamamoto,[c,e] Kiyoshi Takeda[a,b,f]

Department of Microbiology and Immunology, Graduate School of Medicine,[a] Laboratory of Mucosal Immunology,[b] and Laboratory of Immunoparasitology,[c] WPI Immunology Frontier Research Center, Osaka University, Osaka, Japan; Department of Molecular Virology[d] and Department of Immunoparasitology,[e] Research Institute for Microbial Diseases, Osaka University, Osaka, Japan; Core Research for Evolutional Science and Technology, Japan Science and Technology Agency, Saitama, Japan[f]

The interferon-inducible protein with tetratricopeptide (IFIT) family proteins inhibit replication of some viruses by recognizing several types of RNAs, including 5′-triphosphate RNA and 5′ capped 2′-O unmethylated mRNA. However, it remains unclear how IFITs inhibit replication of some viruses through recognition of RNA. Here, we analyzed the mechanisms by which Ifit1 exerts antiviral responses. Replication of a Japanese encephalitis virus (JEV) 2′-O methyltransferase (MTase) mutant was markedly enhanced in mouse embryonic fibroblasts and macrophages lacking Ifit1. Ifit1 bound 5′-triphosphate RNA but more preferentially associated with 5′ capped 2′-O unmethylated mRNA. Ifit1 inhibited the translation of mRNA and thereby restricted the replication of JEV mutated in 2′-O MTase. Thus, Ifit1 inhibits replication of MTase-defective JEV by inhibiting mRNA translation through direct binding to mRNA 5′ structures.

mRNA has a 5′ cap structure, in which the N-7 position of the guanosine residue is methylated. The 5′ cap structure is known to be responsible for the stability and efficient translation of mRNA (1, 2). In higher eukaryotes, the first one or two 5′ nucleotides are additionally methylated at the ribose 2′-O position by distinct host nuclear 2′-O methyltransferases (MTases) (3, 4). However, the functional role of 2′-O methylation (2′-O Me) remains poorly understood. Several viruses that replicate in the cytoplasm possess their own mRNA capping machineries (5–10). For positive-stranded flaviviruses, nonstructural protein 3 (NS3) acts as an RNA 5′-triphosphatase and NS5 possesses both N-7 and 2′-O MTase activities (8, 11, 12). Recent studies have revealed that 2′-O methylation of the mRNA 5′ cap in these viruses is important for evasion from the host innate immune responses (13–15). However, the 2′-O MTase activity has been shown to be absent from several paramyxoviruses, such as Newcastle disease virus (NDV) and respiratory syncytial virus (RSV) (16, 17).

Type I interferons (IFNs) induce the expression of a large number of antiviral genes through a Janus kinase/signal transducer and activator of transcription (JAK/STAT) pathway (18, 19). Among the IFN-inducible genes, the IFN-inducible protein with tetratricopeptide (IFIT) genes comprise a large family with three (*Ifit1*, *Ifit2*, and *Ifit3*) and four (*IFIT1*, *IFIT2*, *IFIT3*, and *IFIT5*) members in mice and humans, respectively. The murine and human genes are clustered in loci on chromosomes 19C1 and 10q23, respectively (20). IFIT family proteins reportedly associate with several host proteins to exert various cellular functions (21, 22). For example, human IFIT1/IFIT2 and murine Ifit1/Ifit2 bind to eukaryotic translational initiation factor 3 (eIF3) subunits to inhibit translation (23–26). IFIT1 has been suggested to interact with STING/MITA to negatively regulate IRF3 activation (27), whereas IFIT3 may bind TBK1 to enhance type I IFN production and with JAB1 to inhibit leukemia cell growth (28, 29).

In addition to binding host factors, IFIT proteins have functional effects by interacting directly with products of viruses. Human IFIT1 interacts with the human papillomavirus E1 protein and human IFIT2 interacts with the AU-rich RNA of NDV to exert antiviral effects (30, 31). Direct binding of IFIT proteins to virus RNA has also been demonstrated in several recent studies. IFIT1 and IFIT5 bind to the 5′-triphosphate (5′-PPP) RNA that is present in the genomes of viruses (32, 33). Structural studies of human IFIT2 and human IFIT5 identified an RNA-binding site and defined the structural basis of a complex with 5′-PPP RNA (31, 33). However, these structural studies did not explain how IFIT binds to or restricts virus RNA that has a 5′ cap but lacks methylation at the 2′-O position (13–15). Thus, it remains unclear how IFITs mediate antiviral activities against viruses that have a 5′ cap but lack 2′-O MTase activity.

In this study, we analyzed the mechanisms by which murine Ifit1 exerts the host defense against a flavivirus lacking 2′-O MTase activity. Ifit1 was found to preferentially interact with 5′ capped mRNA without 2′-O methylation and inhibit its translation. Thus, Ifit1 participates in antiviral responses targeting 5′ capped mRNA without 2′-O methylation.

MATERIALS AND METHODS

Mice. All animal experiments were conducted in accordance with the guidelines of the Animal Care and Use Committee of the Graduate School of Medicine, Osaka University. The gene-targeting strategies for generating *Ifit1*-knockout (*Ifit1*$^{-/-}$) mice were described previously (34). The *Ifit1*-targeting vector was designed to replace a 1.8-kb fragment encoding the exon of *Ifit1* with a neomycin resistance gene cassette (Neo). A short arm and a long arm of the homology region from the v6.5 embryonic stem (ES) cell genome were amplified by PCR. A herpes simplex virus (HSV) thymidine kinase (tk) gene was inserted into the 3′ end of the vector. After the *Ifit1*-targeting vector was electroporated into ES cells, G418 and ganciclovir doubly resistant clones were selected and screened by PCR and

Received 2 April 2013 Accepted 26 June 2013
Published ahead of print 3 July 2013
Address correspondence to Kiyoshi Takeda, ktakeda@ongene.med.osaka-u.ac.jp.

doi:10.1128/JVI.00883-13

Southern blot analysis. An ES cell clone correctly targeting *Ifit1* was microinjected into C57BL/6 mouse blastocysts. Chimeric mice were mated with female C57BL/6 mice, and heterozygous F1 progenies were intercrossed to obtain *Ifit1*$^{-/-}$ mice.

Cells. HEK293T cells, Vero cells, and mouse embryonic fibroblasts (MEFs) were maintained in Dulbecco's modified Eagle's medium (Nakalai Tesque) supplemented with 10% fetal bovine serum (JRH Bioscience), 100 U/ml penicillin, and 100 μg/ml streptomycin (Gibco). MEFs were prepared from wild-type (WT) and *Ifit1*$^{-/-}$ day 14.5 embryos and immortalized by introduction of a plasmid encoding the simian virus 40 large T antigen. MEFs stably expressing Ifit1 were established by the previously described method with some modifications (34). In short, full-length cDNA of *Ifit1* was cloned into pMRX-puro (pMRX/*Ifit1*). Retrovirus was produced by introduction of pMRX/*Ifit1* into Plat-E packaging cells (35). MEFs were infected with the retrovirus, cultured in the presence of 1 μg/ml of puromycin (Sigma) for 5 days, and harvested for subsequent studies. To isolate peritoneal macrophages, mice were intraperitoneally injected with 5 ml of 4% thioglycolate medium (Sigma), and peritoneal exudative cells were isolated from the peritoneal cavity at 3 days postinjection. The cells were incubated for 2 h and then washed three times with Hanks' balanced salt solution. The remaining adherent cells were used as peritoneal macrophages in the experiments.

Viruses. Japanese encephalitis virus (JEV) strain AT31 (36) was used for the experiments. An NS5 K61A mutation of JEV was introduced into pMWATG1 (37) by PCR-based mutagenesis with the primers 5′-GCGAGGCTCAGCAGCTCTCCGTTGGCTCG-3′ and 5′-CGAGCCAACGGAGAGCTGCTGAGCCTCGC-3′ (the mutagenesis site is underlined) and verified by DNA sequencing. A recombinant virus, the JEV K61A mutant, was generated from pMWJEATG1/JEV K61A as previously described (36). MEFs or macrophages were infected with JEV at specified multiplicities of infection (MOIs). The virus yields in the culture supernatants were titrated by focus-forming assays on Vero cells and expressed as the number of focus-forming units (FFU), as previously described (38). The virus RNA accumulations in the JEV-infected cells were determined by real-time reverse transcription-PCR (RT-PCR) with primers targeting JEV NS5, normalized to the level of host GAPDH (glyceraldehyde-3-phosphate dehydrogenase), and expressed as the fold change in *Ifit1*$^{-/-}$ cells versus wild-type cells (value for wild type = 1).

Preparation of RNA. The 5′-terminal 200 nucleotides of the JEV genome were amplified by PCR using pMWATG1 (37) with the primers 5′-TAATACGACTCACTATTAGAAGTTTATCT-3′ (the T7 class II promoter sequence is underlined) and 5′-CATTACTACCCTCTTCACTCCCACTAGTGG-3′, and the luciferase reporter gene (*luc2*) was amplified using pGL4.14 (Promega) with the primers 5′-TAATACGACTCACTATAGGCCACCATGGAAGATGCCAAAAA-3′ (the T7 class III promoter sequence is underlined) and 5′-TACCACATTTGTAGAGGTTTTACTTGCTTT-3′. Subsequently, the PCR products were *in vitro* transcribed under the control of the T7 promoter with MEGAScript (Ambion). Biotin-labeled RNA was prepared by *in vitro* transcription in the presence of biotin-labeled UTP (PerkinElmer). Capped RNA substrates were produced with a ScriptCap 7-methylguanosine (m7G) capping system (Epicentre) in the presence (5′ cap positive [5′ cap$^+$]/2′-O Me positive [2′-O Me$^+$]) or absence (5′ cap$^+$/2′-O Me negative [2′-O Me$^-$]) of a ScriptCap vaccinia virus 2′-O MTase (Epicentre). ^{32}P-labeled m7GpppA-RNA substrate was prepared with a ScriptCap m7G capping system in the presence of ^{32}P-labeled GTP. A 5′ OH-RNA substrate was produced by incubating *in vitro*-transcribed RNA with calf intestinal alkaline phosphatase (CIAP) for 3 h at 37°C. All RNA substrates were purified with an RNeasy minikit (Qiagen) and stored at −80°C until use.

Real-time RT-PCR. Total RNA was isolated with the TRIzol reagent (Invitrogen), and 1 to 2 μg of RNA was reverse transcribed using Moloney murine leukemia virus reverse transcriptase (Promega) and random primers (Toyobo) after treatment with RQ1 DNase I (Promega). Real-time RT-PCR was performed in an ABI 7300 apparatus (Applied Biosystems) using a GoTaq real-time PCR system (Promega). All values were normalized by the expression of the GAPDH gene. The following primer sets were used: for the JEV NS5 gene, 5′-AACGCACATTACGCGTCCTAGAGATGA-3′ and 5′-CTAACCCAATACATCTCGTGATTGGAGTT-3′; for *Ifnb*, 5′-GGAGATGACGGAGAAGATGC-3′ and 5′-CCCAGTGCTGGAGAAATTGT-3′; for *luc2*, 5′-CCATTCTACCCACTCGAAGACG-3′ and 5′-CGTAGGTAATGTCCACCTCGA-3′; and for the GAPDH gene, 5′-CCTCGTCCCGTAGACAAAATG-3′ and 5′-TCTCCACTTTGCCACTGCAA-3′.

Recombinant proteins. Wild-type and K61A mutant JEV N-terminal NS5 (MTase domain) cDNAs were obtained by PCR using pMWATG1 with the primers 5′-GGATCCGGAAGGCCTGGGGGCAGGACGCTA-3′ and 5′-CTCGAGATGCTCAGGGTCTTTGTGCCACGT-3′. Full-length murine *Ifit1* cDNA and JEV MTase cDNA were inserted into pET-15b and pGEX-6P, respectively. pET/*Ifit1* and pGEX/JEV MTases were transformed into the *Escherichia coli* BL21(DE3) strain. Expression of the Ifit1 and JEV NS5 proteins was induced by addition of 0.5 mM isopropyl-1-thio-β-D-galactopyranoside (IPTG), and the expressed Ifit1 and JEV MTase proteins were purified using Ni^{2+}-affinity chromatography (Novagen) and glutathione-Sepharose 4B (Amersham Biosciences), respectively, according to each manufacturer's instructions. The purified protein was desalted and concentrated using an Amicon Ultra centrifugal filter unit (Millipore) and stored at −80°C until use.

***In vitro* MTase activity assay.** The MTase reaction was performed in a 20-μl reaction mixture of 50 mM Tris-HCl (pH 8.0), 6 mM KCl, 1.25 mM $MgCl_2$, and 0.5 mM *S*-adenosylmethionine (AdoMet) containing 10 nmol of ^{32}P-labeled m7GpppA-RNA substrate (JEV 5′-terminal 200 nucleotides) and 30 pmol of JEV MTase or 80 units of vaccinia virus 2′-O MTase (Epicentre) for 3 h at 37°C. The RNA was purified by passage through a postreaction cleanup column (Sigma) and digested with 10 U of nuclease P1 (Wako) in 50 mM sodium acetate overnight at 37°C. The samples were analyzed on thin-layer chromatography polyethyleneimine (PEI)-cellulose plates developed with 0.3 M ammonium sulfate.

RNA EMSAs. RNA electrophoretic mobility shift assays (EMSAs) were performed using a LightShift chemiluminescent RNA EMSA kit (Thermo Scientific) according to the manufacturer's instructions. Briefly, 0 to 20 pmol of recombinant murine Ifit1 and 2.5 pmol of *in vitro*-transcribed and biotin-labeled RNA were coincubated for 30 min at room temperature in RNA EMSA binding buffer (10 mM HEPES, pH 7.3, 20 mM KCl, 1 mM $MgCl_2$, 1 mM dithiothreitol, 0.1 μg/μl of yeast tRNA, 2% glycerol). The resulting Ifit1/RNA complexes were electrophoresed in a 7.5% native polyacrylamide gel. The separated RNAs were transferred to a positively charged nylon membrane and cross-linked at 120 mJ/cm^2 and an absorbance of 254 nm. The membrane was incubated with stabilized streptavidin-horseradish peroxidase conjugate (1:300 dilution; a component of the EMSA kit), and the bound stable peroxide was detected with luminol/enhancer solution (another component of the EMSA kit). The gel-shift band intensities were quantified using ImageJ software (National Institutes of Health).

RNA pulldown assay. For RNA pulldown assays, an expression vector for hemagglutinin (HA)-tagged murine full-length Ifit1 was transfected into HEK293T cells using Lipofectamine 2000 (Invitrogen). The *Ifit1*-transfected cells were lysed in RNA-binding buffer (10 mM HEPES, pH 7.3, 500 mM KCl, 1 mM EDTA, 2 mM $MgCl_2$, 0.1% NP-40, 0.1 μg/μl of yeast tRNA (Ambion), 1 U/ml of RNase inhibitor [Toyobo]), and the lysate (200 μg) was coincubated with 25 pmol of biotin-labeled RNA and streptavidin-agarose (Invitrogen) in RNA-binding buffer for 30 min at room temperature. The binding complexes were washed five times with RNA-binding buffer, followed by SDS-PAGE and immunoblotting with an anti-HA probe (F-7) antibody (Santa Cruz Biotechnology). The intensity of the detected Ifit1 band was quantified using ImageJ software (National Institutes of Health).

RNA immunoprecipitation. RNA immunoprecipitation was performed as described previously (38) with slight modifications. MEFs (2×10^5) stably expressing Flag-tagged Ifit1 were infected with JEV at an MOI of 1.0 and cultured for 24 h. The cells were then lysed in 500 μl of RNA

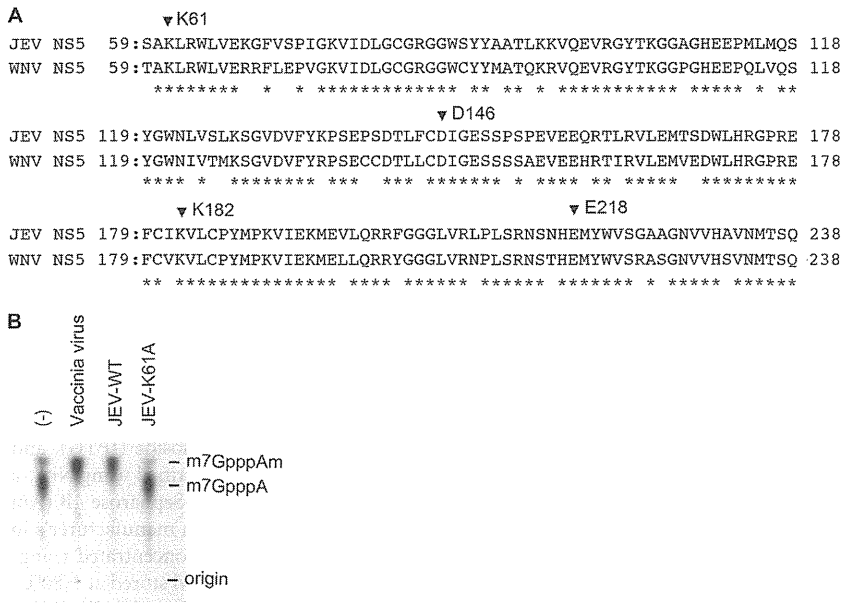

FIG 1 Generation of an MTase-defective JEV mutant. (A) Sequence homology between NS5 proteins of JEV (AT31 strain, GenBank accession number AB196926) and WNV (00-3356 strain, GenBank accession number EF530047). Arrowheads, MTase catalytic K-D-K-E tetrad; *, consensus sequences between the two proteins. (B) 2′-O MTase activity of JEV WT and JEV K61A mutant recombinant NS5 proteins by thin-layer chromatography assays. The substrate m7GpppA-RNA (^{32}P-labeled JEV 5′-terminal 200 nucleotides) was methylated *in vitro* with the respective recombinant NS5 proteins or vaccinia virus 2′-O MTase, digested with P1 nuclease, and developed on PEI-cellulose plates. The positions of 2′-O methylated (m7GpppAm) and unmethylated (m7GpppA) RNA are indicated. Data are representative of four independent experiments.

buffer (10 mM HEPES, pH 7.3, 500 mM KCl, 1 mM EDTA, 2 mM $MgCl_2$, 0.1% NP-40, 0.1 μg/μl of yeast tRNA (Ambion), 1 U/ml of RNase inhibitor [Toyobo], 1 tablet/10 ml of Complete mini-protease inhibitor cocktail [Roche]). After centrifugation at 15,000 rpm for 20 min at 4°C, 50-μl aliquots of the supernatants were recovered as input samples and the remaining supernatants were precleared with 30 μl of 50% protein G-conjugated Sepharose and 1 μg of mouse normal IgG for 1 h. After centrifugation of the beads, the supernatants were immunoprecipitated with 1 μg of mouse normal IgG or anti-Flag M2 antibody (Santa Cruz Biotechnology) and 30 μl of 50% protein G-conjugated Sepharose. The beads were washed five times with RNA buffer without yeast tRNA, and RNA was isolated from the precipitants and input samples with the TRIzol reagent. The RNA was reverse transcribed as described above and subjected to the first round of PCR with JEV NS1-specific primers 5′-TCTG TCACTAGACTGGAGCA-3′ and 5′-CCAGAAACATCACCAGAAGG-3′. The PCR products were then analyzed by quantitative PCR with nested primers 5′-GAGCACTGACGAGTGTGATG-3′ and 5′-AGCGACTCTC AATCCAGTAC-3′. All values were normalized by the values for the input samples (indicated as percent input).

Cellular translational reporter assay. MEFs (2×10^5) were pretreated with 1,000 U/ml of universal type I interferon (PBL Biomedical Laboratories) for 6 h. Three types of 5′ modified luciferase mRNAs (2 μg of 5′-PPP, 5′ cap$^+$/2′-O Me$^-$, and 5′ cap$^+$/2′-O Me$^+$) were transiently transfected into MEFs using the Lipofectamine 2000 reagent (Invitrogen) according to the manufacturer's instructions. At 6 h after the transfection, RNA was isolated and analyzed for the quantity of the luciferase mRNAs (*luc2*). The luciferase activities of whole-cell lysates were measured using a dual-luciferase reporter assay system (Promega). The numbers of relative light units (RLU) were normalized by the concentrations of proteins determined by use of a bicinchoninic acid protein assay kit (Thermo Scientific).

Statistical analysis. Statistical analyses were conducted on each independent data set. An unpaired Student's *t* test was used to determine the statistical significance of differences in the experimental data. *P* values of <0.05 were considered to indicate statistical significance.

RESULTS

***Ifit1*$^{-/-}$ cells fail to restrict the replication of a mutant JEV lacking 2′-O MTase activity.** Previous analysis of the flavivirus West Nile virus (WNV) 2′-O MTase revealed residues in NS5 (K61, D146, K182, and E218) that were essential for its biochemical activity (8). A WNV mutant (E218A) lacking 2′-O MTase activity was attenuated in mouse MEFs and macrophages but showed enhanced replication in *Ifit1*$^{-/-}$ cells (13, 15). As NS5 is a highly conserved protein in flaviviruses, the four residues integral to the 2′-O MTase activity are identical in WNV and JEV (Fig. 1A). Replacement of lysine 61 by alanine in the JEV NS5 MTase domain (JEV K61A) abolished the JEV 2′-O MTase activity *in vitro* (Fig. 1B). We generated *Ifit1*$^{-/-}$ mice (Fig. 2A to C) and infected MEFs with JEV WT and JEV K61A strains (Fig. 3A). The JEV WT replicated equivalently in wild-type and *Ifit1*$^{-/-}$ MEFs. In comparison, the production of the JEV K61A mutant was decreased in wild-type MEFs, suggesting that 2′-O MTase activity is required for JEV replication. Consistent with this and analogous studies with an WNV E218A strain (13), replication of the JEV K61A strain was enhanced (approximately 173-fold increased at 4 days postinfection; $P < 0.05$) in *Ifit1*$^{-/-}$ MEFs compared with wild-type MEFs. We also infected peritoneal macrophages with JEV WT and JEV K61A strains (Fig. 3B). Similar to the results obtained with MEFs, replication of the JEV WT was similarly observed in wild-type and *Ifit1*$^{-/-}$ macrophages. However, replication of the JEV K61A mutant was severely decreased in wild-type but not *Ifit1*$^{-/-}$ macrophages, and the virus was not detected at 4 days postinfection in wild-type cells. For further confirmation, we analyzed virus RNA accumulation at 4 days postinfection (Fig. 3C and D). Whereas RNA levels of JEV WT were similar in wild-type and *Ifit1*$^{-/-}$ MEFs, those of the JEV K61A mutant were markedly

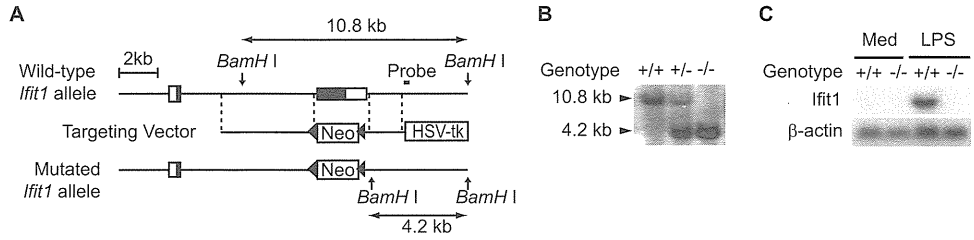

FIG 2 Generation of *Ifit1*$^{-/-}$ mice. (A) Schematic representation of the *Ifit1* gene-targeting strategies. Solid boxes, coding regions of the *Ifit1* gene; open boxes, untranslated regions; Neo and HSV tk, a neomycin-resistance gene cassette and a herpes simplex virus thymidine kinase gene, respectively. The positions of the probe and restriction enzyme site for Southern blotting are shown. (B) Genomic DNA was isolated from the tails of wild-type (+/+), heterozygous (+/-), and homozygous (−/−) *Ifit1* mutant mice. A Southern blot analysis performed after digestion of the genomic DNA with BamHI shows the correct targeting of the locus. (C) Peritoneal exudative macrophages were harvested from wild-type (+/+) or *Ifit1*-deficient (−/−) mice. Total RNA (10 μg) was blotted onto a nylon membrane, and Ifit1 and β-actin mRNA expression was detected by Northern blot analysis with the respective cDNA probes. LPS lanes, cells stimulated with 100 ng/ml of lipopolysaccharide for 4 h to induce endogenous Ifit1 expression; Med lanes, cells treated with medium alone.

higher (approximately 13-fold; $P < 0.05$) in *Ifit1*$^{-/-}$ MEFs than in wild-type MEFs. To further corroborate these findings, we reintroduced the *Ifit1* gene into *Ifit1*$^{-/-}$ MEFs using a retrovirus vector. Replication of the JEV K61A mutant was considerably suppressed (approximately 4-fold; $P < 0.05$) by ectopic Ifit1 expression in *Ifit1*$^{-/-}$ MEFs (Fig. 3E). *Ifnb* was similarly induced in wild-type and *Ifit1*$^{-/-}$ MEFs after infection with the JEV K61A mutant, excluding the possibility that defective type I IFN production is responsible for the high sensitivity to infection with the JEV K61A mutant in *Ifit1*$^{-/-}$ cells (Fig. 3F). Thus, consistent with the findings of previous studies (13, 15), Ifit1 inhibits replication and infection of flavivirus mutants that lack 2′-O MTase activity.

Ifit1 preferentially binds to virus RNA lacking 2′-O methylation. Next, we analyzed how Ifit1 recognizes 2′-O MTase mutant

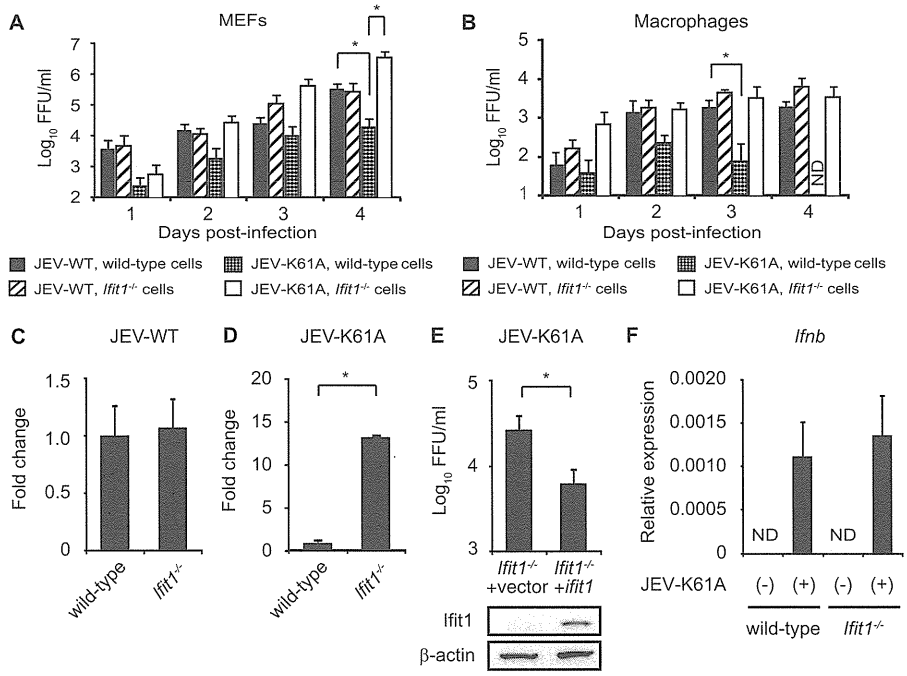

FIG 3 *Ifit1*$^{-/-}$ MEFs and macrophages fail to restrict the replication of the 2′-O MTase mutant JEV. (A, B) Culture supernatants of wild-type and *Ifit1*$^{-/-}$ MEFs (A) and macrophages (B) infected with JEV WT and the JEV K61A mutant (MOIs, 0.1 for MEFs and 0.5 for macrophages) were harvested at the indicated days postinfection. The virus titers in 1-ml supernatant aliquots were determined by focus-forming assays on Vero cells and expressed as the $\log_{10}$ number of FFU/ml. Data are shown as means ± SDs of quadruplicate samples generated from four independent experiments with statistical significance. ND, not detected. *, $P < 0.05$. (C, D) Accumulation of JEV WT (C) and the JEV K61A mutant (D) RNA in wild-type and *Ifit1*$^{-/-}$ MEFs at 4 days postinfection determined by quantitative real-time RT-PCR. JEV NS5 RNA levels were normalized to the level of host GAPDH and are expressed as the fold change in *Ifit1*$^{-/-}$ cells versus wild-type cells (value for wild type = 1). Data are representative of three independent experiments with statistical significance. *, $P < 0.05$. (E) Culture supernatants of vector-transduced (+vector) and Flag-tagged *Ifit1* gene-transduced (+*Ifit1*) *Ifit1*$^{-/-}$ MEFs infected with the JEV K61A mutant (MOI, 0.1) were harvested at 3 days postinfection. The virus titers in 1-ml supernatant aliquots were determined by focus-forming assays on Vero cells and expressed as the $\log_{10}$ number of FFU/ml. Expression of Ifit1 and β-actin determined by immunoblotting with anti-Flag or anti-β-actin antibodies is shown at the bottom. Data are representative of three independent experiments. *, $P < 0.05$. (F) Wild-type and *Ifit1*$^{-/-}$ MEFs were infected with the JEV K61A mutant (MOI, 0.1). At 4 days postinfection, cells were harvested and analyzed for *Ifnb* expression by quantitative RT-PCR. *Ifnb* RNA levels were expressed relative to those of GAPDH. ND, not detected. Data are shown as means ± SDs and are representative of data from three independent experiments.

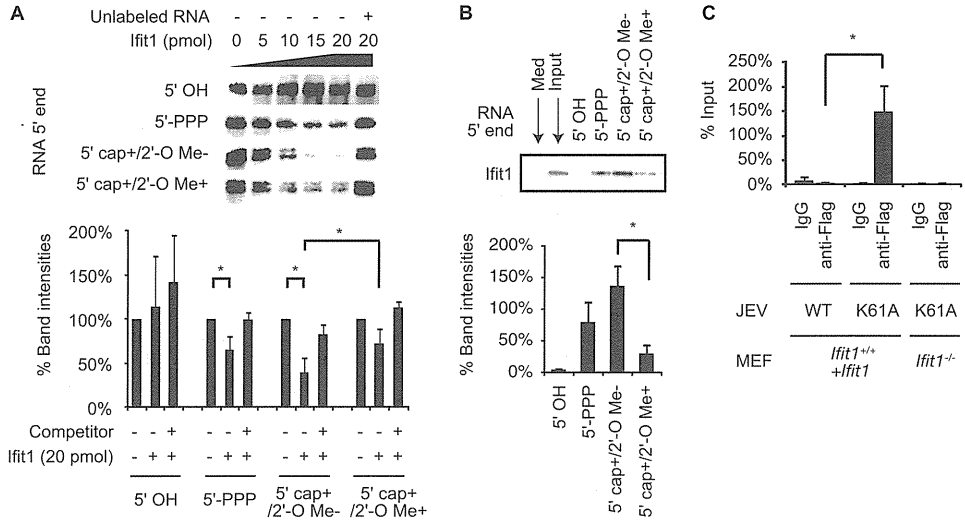

FIG 4 Ifit1 preferentially binds to virus RNA lacking 2′-O methylation. (A) Electrophoretic mobility shift of biotin-labeled RNA (JEV 5′-terminal 200 nucleotides) with recombinant Ifit1. The presence or absence of a 5′ cap and 2′-O Me of the JEV 5′-terminal 200 nucleotides is indicated. Unlabeled 5′-PPP RNA was used as a competitor. The loss of the band indicates binding of RNA and Ifit1 (top). The band intensities (in percent) calculated by ImageJ are shown at the bottom. Data are representative (top) and means ± SDs (bottom) of five independent experiments. *, $P < 0.05$. (B) Lysates from HEK293T cells transfected with HA-tagged Ifit1 were incubated with 2.5 pmol of biotin-labeled RNA. The presence or absence of a 5′ cap and 2′-O Me of the JEV 5′-terminal 200 nucleotides is indicated. 5′ OH RNA was produced by incubating *in vitro*-transcribed RNA with CIAP. RNA was incubated with streptavidin beads, and the precipitates were separated by SDS-PAGE and immunoblotted with an anti-HA antibody (top). Med and Input, samples from whole-cell lysates of empty vector- and *Ifit1*-transfected 293T cells, respectively. The percent band intensities calculated by ImageJ are shown at the bottom. Data are representative (top) and means ± SDs (bottom) of three independent experiments. *, $P < 0.05$. (C) MEFs stably expressing Ifit1 ($Ifit1^{+/+}$ + *Ifit1*) or $Ifit1^{-/-}$ MEFs were infected with JEV WT or the JEV K61A mutant at an MOI of 1.0. The cells were harvested after 24 h, and JEV RNA/Ifit1-binding complexes were immunoprecipitated with a mouse anti-Flag antibody or mouse IgG. The immunoprecipitated RNA was analyzed by nested RT-PCR using primers that detect the JEV NS1 gene. Each value was normalized by the value for the input (indicated in percent). Data are means ± SDs of three independent experiments. *, $P < 0.05$.

viruses. While recombinant IFIT1 reportedly binds to 5′-PPP RNA (32), the mRNA of the JEV K61A mutant has a 5′ m7G cap but lacks 2′-O methylation (5′ cap$^+$/2′-O Me$^-$). We examined whether Ifit1 can also interact directly with 5′ cap$^+$/2′-O Me$^-$ RNA using electrophoretic mobility shift assays. Consistent with a previous report (32), bands of 5′-PPP RNA but not RNA lacking phosphate at the 5′ end (5′ OH) were diminished after addition of recombinant Ifit1 (Fig. 4A). Furthermore, Ifit1 blocked the electrophoretic mobility of the 5′ cap$^+$/2′-O Me$^-$ RNA. However, this effect was rescued by exogenous addition *in vitro* of 2′-O methylation (5′ cap$^+$/2′-O Me$^+$). The efficient binding of Ifit1 to 5′ cap$^+$/2′-O Me$^-$ RNA was corroborated by RNA pulldown assays (Fig. 4B). HA-tagged Ifit1 was expressed in HEK293T cells, and cell lysates were incubated with biotin-labeled *in vitro*-transcribed RNA and streptavidin-agarose. Then, binding complexes of Ifit1/RNA were analyzed by Western blotting. While Ifit1 was not pulled down with 5′ OH RNA, modest binding of Ifit1 to 5′-PPP RNA and 5′ cap$^+$/2′-O Me$^+$ RNA was observed. In comparison, the strongest Ifit1 protein signal was observed with 5′ cap$^+$/2′-O Me$^-$ RNA. These findings suggest that Ifit1 preferentially binds to 5′ capped RNA lacking 2′-O methylation.

To confirm independently that Ifit1 interacts with 5′ capped RNA lacking 2′-O methylation, we performed RNA immunoprecipitation assays using cell lysates from JEV-infected MEFs that ectopically expressed a Flag-tagged Ifit1. After immunoprecipitation with an anti-Flag antibody, the JEV mRNA was measured by nested RT-PCR analysis (Fig. 4C). JEV RNA was only marginally detected in lysates precipitated with control IgG and lysates of $Ifit1^{-/-}$ MEFs infected with the JEV K61A mutant, indicating the specificity of Ifit1 binding in the assay. Virus RNA in JEV K61A mutant-infected MEFs was detected at a level over 37-fold higher than that in JEV WT-infected MEFs. Taken together, these findings suggest that Ifit1 directly interacts with virus mRNA lacking 2′-O methylation.

Ifit1 selectively inhibits translation of 5′ capped 2′-O unmethylated mRNA. To examine the mechanism by which Ifit1 exerts an antiviral effect by associating with mRNA lacking 2′-O methylation, we used a luciferase translational reporter assay. Luciferase RNAs with different 5′ structures were transfected into type I IFN-primed MEFs, and total RNA and cell lysates were harvested 6 h later. Importantly, the levels of luciferase RNAs in wild-type and $Ifit1^{-/-}$ cells were unaffected by any of the 5′ modifications (Fig. 5A). We then analyzed the translational efficiency of the transfected RNAs by measuring the luciferase activity (Fig. 5B). As expected (1), uncapped 5′-PPP luciferase mRNA was not translated in either wild-type or $Ifit1^{-/-}$ MEFs. Capping of the mRNA (5′ cap$^+$/2′-O Me$^-$) increased translation in wild-type cells, although the levels were profoundly lower ($P < 0.05$) than those in $Ifit1^{-/-}$ cells. In comparison, addition of 2′-O methylation to the 5′ cap (5′ cap$^+$/2′-O Me$^+$) *in vitro* resulted in similar levels of translation in wild-type and $Ifit1^{-/-}$ MEFs. Even in MEFs that were not treated with type I IFN, similar patterns of luciferase activity were observed (Fig. 5C), indicating that slightly expressed Ifit1 might contribute to the inhibition. Taken together, our data establish that Ifit1 preferentially binds to 5′ capped mRNA lacking 2′-O methylation and inhibits its translation.

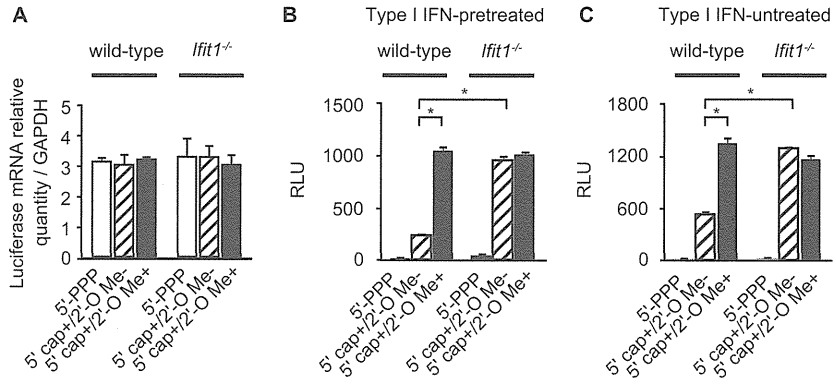

FIG 5 Ifit1 selectively inhibits the translation of mRNA lacking 2′-O methylation. (A) The luciferase RNA amounts at 6 h after RNA transfection were determined by quantitative real-time RT-PCR. The relative luciferase mRNA amounts, calculated as the amount of each transfected mRNA (*luc2*) divided by the level of GAPDH mRNA expression, are shown. The presence or absence of a 5′ cap and 2′-O Me of the introduced luciferase RNA is indicated. Data are shown as means ± SDs and are representative of three independent experiments. (B, C) Wild-type and *Ifit1*$^{-/-}$ MEFs pretreated with type I IFN (B) or untreated (C) were transiently transfected with luciferase mRNA. Luciferase activities were measured at 6 h after the transfection and are shown as relative light units (RLU). The presence or absence of a 5′ cap and 2′-O Me of the introduced luciferase RNA is indicated. Data are shown as means ± SDs of triplicate samples of the representative results. Similar results were obtained in three independent experiments. *, $P < 0.05$.

DISCUSSION

In this study, we investigated the mechanisms by which Ifit1 recognizes RNA of JEV lacking 2′-O MTase activity. Ifit1 inhibited the translation of mRNA through association with mRNA lacking 2′-O methylation.

To analyze the role of Ifit1 in 5′ cap structure-dependent antiviral responses, we generated a JEV MTase mutant. The K61, D146, K182, and E218 residues have all been shown to be essential for the MTase activity of the NS5 protein and replication of WNV (8, 11). While a WNV E218A mutant was previously used for analysis of Ifit1-mediated antiviral responses (13), in our assays, the corresponding JEV E218A mutant was severely impaired in replication in Vero cells and rapidly reverted to the wild type during cell culture, preventing its use (data not shown). A similar phenotype was observed with the WNV D146A 2′-O methylation mutant (11). However, unlike our results, it has recently been reported that a JEV E218A mutant is stable in Vero cells (39). This would be due to the different strains used in the two studies. Thus, mutation of residues that are essential for the 2′-O MTase activity of a flavivirus NS5 protein can differentially impact replication of JEV and WNV even in cells lacking type I IFN responses and IFIT1 expression.

Previous *in vitro* studies indicated that IFIT family proteins bind to several types of RNA, including 5′-PPP RNA and AU-rich double-stranded RNA (31, 32). Indeed, an analysis of the IFIT2 crystal structure indicated the presence of a positively charged RNA-binding channel (31), findings which were supported by the X-ray crystallographic structure of complexes of 5′-PPP RNA with human IFIT5 (33, 40). We also observed that Ifit1 could bind to 5′-PPP RNA. However, our biochemical analysis showed that Ifit1 bound strongly to 5′ capped RNA lacking 2′-O methylation and addition of 2′-O methylation weakened the binding of Ifit1 to the RNA. Since mRNAs of virtually all higher eukaryotes are believed to be methylated at the ribose 2′-O position (41), this modification likely serves as a molecular pattern for discriminating self from nonself.

Although it remains unclear how 2′-O methylation reduces Ifit1 binding to RNA, structural changes to the RNA at the 5′ terminus after 2′-O methylation could sterically hamper Ifit1 binding. The crystal structure of the 5′-PPP RNA/IFIT5 complex has indicated that the RNA-binding site on human IFIT5 is located in a narrow pocket, thus raising the possibility that 5′ capped and 2′-O methylated RNA cannot fit within an analogous pocket of Ifit1 due to a size limitation (33). Future structural analyses of the binding complex of 5′ capped RNA with Ifit1 will be required to reveal the precise mechanisms by which Ifit1 recognizes 5′ capped RNA lacking 2′-O methylation. Additional studies must also test whether other IFITs preferentially associate with 5′ capped RNA lacking 2′-O methylation.

Ifit1 also has an antiviral activity against several negative-stranded viruses, such as vesicular stomatitis virus (VSV) and parainfluenza virus type 5 (PIV5) (32, 42), whose mRNAs are 2′-O methylated (6, 42). In this regard, Ifit1 is supposed to have an antiviral effect independent of 2′-O methylation. Indeed, IFIT1 is able to bind 5′-PPP genomic RNA (32).

Given the previous and present findings that Ifit1 inhibits mRNA translation (23–26), our data are most consistent with a model in which Ifit1 restricts replication of viruses with 5′ capped RNA lacking 2′-O methylation through direct RNA binding and subsequent inhibition of translation. Human IFIT1 and murine Ifit1 were previously reported to interact with eIF3 to interfere with translation (23–26), and replication of hepatitis C virus, whose RNA lacks a 5′ cap, was also impaired by IFIT1 through binding to eIF3 (43). Thus, Ifit1 may associate with both eIF3 and virus mRNA to inhibit translation and infection.

The Ifit family proteins consist of several conserved members. However, Ifit1 and Ifit2 appear to have distinct antiviral activities (44). Thus, the nonredundant and redundant roles of the Ifit family proteins remain to be elucidated. Generation of mice lacking the other members or all of the Ifit family proteins will be useful to reveal the physiological functions.

ACKNOWLEDGMENTS

We thank M. S. Diamond for fruitful discussions and suggestions, T. Wakita for providing us with the JEV AT31 strain, and T. Kitamura for providing us with Plat-E cells. We also thank Y. Magota for technical assistance, C. Hidaka for excellent secretarial assistance, and members of the K. Takeda laboratory for discussions.

This work was supported by grants from the Ministry of Education, Culture, Sports, Science and Technology, the Japan Science and Technology Agency, and The Osaka Foundation for Promotion of Clinical Immunology.

REFERENCES

1. Muthukrishnan S, Both GW, Furuichi Y, Shatkin AJ. 1975. 5′-Terminal 7-methylguanosine in eukaryotic mRNA is required for translation. Nature 255:33–37.
2. Furuichi Y, LaFiandra A, Shatkin AJ. 1977. 5′-Terminal structure and mRNA stability. Nature 266:235–239.
3. Belanger F, Stepinski J, Darzynkiewicz E, Pelletier J. 2010. Characterization of hMTr1, a human Cap1 2′-O-ribose methyltransferase. J. Biol. Chem. 285:33037–33044.
4. Werner M, Purta E, Kaminska KH, Cymerman IA, Campbell DA, Mittra B, Zamudio JR, Sturm NR, Jaworski J, Bujnicki JM. 2011. 2′-O-Ribose methylation of cap2 in human: function and evolution in a horizontally mobile family. Nucleic Acids Res. 39:4756–4768.
5. Both GW, Furuichi Y, Muthukrishnan S, Shatkin AJ. 1975. Ribosome binding to reovirus mRNA in protein synthesis requires 5′ terminal 7-methylguanosine. Cell 6:185–195.
6. Abraham G, Rhodes DP, Banerjee AK. 1975. The 5′ terminal structure of the methylated mRNA synthesized in vitro by vesicular stomatitis virus. Cell 5:51–58.
7. Salas ML, Kuznar J, Vinuela E. 1981. Polyadenylation, methylation, and capping of the RNA synthesized in vitro by African swine fever virus. Virology 113:484–491.
8. Ray D, Shah A, Tilgner M, Guo Y, Zhao Y, Dong H, Deas TS, Zhou Y, Li H, Shi PY. 2006. West Nile virus 5′-cap structure is formed by sequential guanine N-7 and ribose 2′-O methylations by nonstructural protein 5. J. Virol. 80:8362–8370.
9. Decroly E, Imbert I, Coutard B, Bouvet M, Selisko B, Alvarez K, Gorbalenya AE, Snijder EJ, Canard B. 2008. Coronavirus nonstructural protein 16 is a cap-0 binding enzyme possessing (nucleoside-2′O)-methyltransferase activity. J. Virol. 82:8071–8084.
10. Morin B, Coutard B, Lelke M, Ferron F, Kerber R, Jamal S, Frangeul A, Baronti C, Charrel R, de Lamballerie X, Vonrhein C, Lescar J, Bricogne G, Gunther S, Canard B. 2010. The N-terminal domain of the arenavirus L protein is an RNA endonuclease essential in mRNA transcription. PLoS Pathog. 6:e1001038. doi:10.1371/journal.ppat.1001038.
11. Zhou Y, Ray D, Zhao Y, Dong H, Ren S, Li Z, Guo Y, Bernard KA, Shi PY, Li H. 2007. Structure and function of flavivirus NS5 methyltransferase. J. Virol. 81:3891–3903.
12. Dong H, Zhang B, Shi PY. 2008. Flavivirus methyltransferase: a novel antiviral target. Antiviral Res. 80:1–10.
13. Daffis S, Szretter KJ, Schriewer J, Li J, Youn S, Errett J, Lin TY, Schneller S, Zust R, Dong H, Thiel V, Sen GC, Fensterl V, Klimstra WB, Pierson TC, Buller RM, Gale M, Jr, Shi PY, Diamond MS. 2010. 2′-O methylation of the viral mRNA cap evades host restriction by IFIT family members. Nature 468:452–456.
14. Zust R, Cervantes-Barragan L, Habjan M, Maier R, Neuman BW, Ziebuhr J, Szretter KJ, Baker SC, Barchet W, Diamond MS, Siddell SG, Ludewig B, Thiel V. 2011. Ribose 2′-O-methylation provides a molecular signature for the distinction of self and non-self mRNA dependent on the RNA sensor Mda5. Nat. Immunol. 12:137–143.
15. Szretter KJ, Daniels BP, Cho H, Gainey MD, Yokoyama WM, Gale M, Jr, Virgin HW, Klein RS, Sen GC, Diamond MS. 2012. 2′-O methylation of the viral mRNA cap by West Nile virus evades ifit1-dependent and -independent mechanisms of host restriction in vivo. PLoS Pathog. 8:e1002698. doi:10.1371/journal.ppat.1002698.
16. Colonno RJ, Stone HO. 1976. Newcastle disease virus mRNA lacks 2′-O-methylated nucleotides. Nature 261:611–614.
17. Barik S. 1993. The structure of the 5′ terminal cap of the respiratory syncytial virus mRNA. J. Gen. Virol. 74(Pt 3):485–490.
18. Der SD, Zhou A, Williams BR, Silverman RH. 1998. Identification of genes differentially regulated by interferon alpha, beta, or gamma using oligonucleotide arrays. Proc. Natl. Acad. Sci. U. S. A. 95:15623–15628.
19. Takaoka A, Yanai H. 2006. Interferon signalling network in innate defence. Cell. Microbiol. 8:907–922.
20. Fensterl V, Sen GC. 2011. The ISG56/IFIT1 gene family. J. Interferon Cytokine Res. 31:71–78.
21. Sen GC, Fensterl V. 2012. Crystal structure of IFIT2 (ISG54) predicts functional properties of IFITs. Cell Res. 22:1407–1409.
22. Diamond MS, Farzan M. 2013. The broad-spectrum antiviral functions of IFIT and IFITM proteins. Nat. Rev. Immunol. 13:46–57.
23. Hui DJ, Terenzi F, Merrick WC, Sen GC. 2005. Mouse p56 blocks a distinct function of eukaryotic initiation factor 3 in translation initiation. J. Biol. Chem. 280:3433–3440.
24. Terenzi F, Pal S, Sen GC. 2005. Induction and mode of action of the viral stress-inducible murine proteins, P56 and P54. Virology 340:116–124.
25. Terenzi F, Hui DJ, Merrick WC, Sen GC. 2006. Distinct induction patterns and functions of two closely related interferon-inducible human genes, ISG54 and ISG56. J. Biol. Chem. 281:34064–34071.
26. Fensterl V, White CL, Yamashita M, Sen GC. 2008. Novel characteristics of the function and induction of murine p56 family proteins. J. Virol. 82:11045–11053.
27. Li Y, Li C, Xue P, Zhong B, Mao AP, Ran Y, Chen H, Wang YY, Yang F, Shu HB. 2009. ISG56 is a negative-feedback regulator of virus-triggered signaling and cellular antiviral response. Proc. Natl. Acad. Sci. U. S. A. 106:7945–7950.
28. Liu XY, Chen W, Wei B, Shan YF, Wang C. 2011. IFN-induced TPR protein IFIT3 potentiates antiviral signaling by bridging MAVS and TBK1. J. Immunol. 187:2559–2568.
29. Xiao S, Li D, Zhu HQ, Song MG, Pan XR, Jia PM, Peng LL, Dou AX, Chen GQ, Chen SJ, Chen Z, Tong JH. 2006. RIG-G as a key mediator of the antiproliferative activity of interferon-related pathways through enhancing p21 and p27 proteins. Proc. Natl. Acad. Sci. U. S. A. 103:16448–16453.
30. Terenzi F, Saikia P, Sen GC. 2008. Interferon-inducible protein, P56, inhibits HPV DNA replication by binding to the viral protein E1. EMBO J. 27:3311–3321.
31. Yang Z, Liang H, Zhou Q, Li Y, Chen H, Ye W, Chen D, Fleming J, Shu H, Liu Y. 2012. Crystal structure of ISG54 reveals a novel RNA binding structure and potential functional mechanisms. Cell Res. 22:1328–1338.
32. Pichlmair A, Lassnig C, Eberle CA, Gorna MW, Baumann CL, Burkard TR, Burckstummer T, Stefanovic A, Krieger S, Bennett KL, Rulicke T, Weber F, Colinge J, Muller M, Superti-Furga G. 2011. IFIT1 is an antiviral protein that recognizes 5′-triphosphate RNA. Nat. Immunol. 12:624–630.
33. Abbas YM, Pichlmair A, Gorna MW, Superti-Furga G, Nagar B. 2013. Structural basis for viral 5′-PPP-RNA recognition by human IFIT proteins. Nature 494:60–64.
34. Yamamoto M, Okuyama M, Ma JS, Kimura T, Kamiyama N, Saiga H, Ohshima J, Sasai M, Kayama H, Okamoto T, Huang DC, Soldati-Favre D, Horie K, Takeda J, Takeda K. 2012. A cluster of interferon-gamma-inducible p65 GTPases plays a critical role in host defense against Toxoplasma gondii. Immunity 37:302–313.
35. Morita S, Kojima T, Kitamura T. 2000. Plat-E: an efficient and stable system for transient packaging of retroviruses. Gene Ther. 7:1063–1066.
36. Mori Y, Okabayashi T, Yamashita T, Zhao Z, Wakita T, Yasui K, Hasebe F, Tadano M, Konishi E, Moriishi K, Matsuura Y. 2005. Nuclear localization of Japanese encephalitis virus core protein enhances viral replication. J. Virol. 79:3448–3458.
37. Zhao Z, Date T, Li Y, Kato T, Miyamoto M, Yasui K, Wakita T. 2005. Characterization of the E-138 (Glu/Lys) mutation in Japanese encephalitis virus by using a stable, full-length, infectious cDNA clone. J. Gen. Virol. 86:2209–2220.
38. Katoh H, Mori Y, Kambara H, Abe T, Fukuhara T, Morita E, Moriishi K, Kamitani W, Matsuura Y. 2011. Heterogeneous nuclear ribonucleoprotein A2 participates in the replication of Japanese encephalitis virus through an interaction with viral proteins and RNA. J. Virol. 85:10976–10988.
39. Li SH, Dong H, Li XF, Xie X, Zhao H, Deng YQ, Wang XY, Ye Q, Zhu SY, Wang HJ, Zhang B, Leng QB, Zuest R, Qin ED, Qin CF, Shi PY. 2013. Rational design of a flavivirus vaccine by abolishing viral RNA 2′-O methylation. J. Virol. 87:5812–5819.
40. Katibah GE, Lee HJ, Huizar JP, Vogan JM, Alber T, Collins K. 2013. tRNA binding, structure, and localization of the human interferon-induced protein IFIT5. Mol. Cell 49:743–750.
41. Banerjee AK. 1980. 5′-terminal cap structure in eucaryotic messenger ribonucleic acids. Microbiol. Rev. 44:175–205.
42. Andrejeva J, Norsted H, Habjan M, Thiel V, Goodbourn S, Randall RE. 2013. ISG56/IFIT1 is primarily responsible for interferon-induced changes to patterns of parainfluenza virus type 5 transcription and protein synthesis. J. Gen. Virol. 94:59–68.
43. Wang C, Pflugheber J, Sumpter R, Jr, Sodora DL, Hui D, Sen GC, Gale M, Jr. 2003. Alpha interferon induces distinct translational control programs to suppress hepatitis C virus RNA replication. J. Virol. 77:3898–3912.
44. Fensterl V, Wetzel JL, Ramachandran S, Ogino T, Stohlman SA, Bergmann CC, Diamond MS, Virgin HW, Sen GC. 2012. Interferon-induced Ifit2/ISG54 protects mice from lethal VSV neuropathogenesis. PLoS Pathog. 8:e1002712. doi:10.1371/journal.ppat.1002712.

Journal of proteome research

Article

pubs.acs.org/jpr

Understanding the Biological Context of NS5A–Host Interactions in HCV Infection: A Network-Based Approach

Lokesh P. Tripathi,*[,¶,†] Hiroto Kambara,[¶,‡] Yi-An Chen,[†] Yorihiro Nishimura,[‡] Kohji Moriishi,[‡] Toru Okamoto,[‡] Eiji Morita,[‡] Takayuki Abe,[‡] Yoshio Mori,[‡] Yoshiharu Matsuura,[‡] and Kenji Mizuguchi*[,†,§]

[†]National Institute of Biomedical Innovation, 7-6-8 Saito Asagi, Ibaraki, Osaka, 567-0085, Japan

[‡]Department of Molecular Virology, Research Institute for Microbial Diseases, Osaka University, 3-1 Yamada-Oka, Suita, Osaka, 565-0871, Japan

[§]Graduate School of Frontier Biosciences, Osaka University, 1-3 Yamada-Oka, Suita, Osaka, 565-0871, Japan

Supporting Information

ABSTRACT: Hepatitis C virus (HCV) is a major cause of chronic liver disease. HCV NS5A protein plays an important role in HCV infection through its interactions with other HCV proteins and host factors. In an attempt to further our understanding of the biological context of protein interactions between NS5A and host factors in HCV pathogenesis, we generated an extensive physical interaction map between NS5A and cellular factors. By combining a yeast two-hybrid assay with comprehensive literature mining, we built the NS5A interactome composed of 132 human proteins that interact with NS5A. These interactions were integrated into a high-confidence human protein interactome (HPI) with the help of the TargetMine data warehouse system to infer an overall protein interaction map linking NS5A with the components of the host cellular networks. The NS5A–host interactions that were integrated with the HPI were shown to participate in compact and well-connected cellular networks. Functional analysis of the NS5A "infection" network using TargetMine highlighted cellular pathways associated with immune system, cellular signaling, cell adhesion, cellular growth and death among others, which were significantly targeted by NS5A–host interactions. In addition, cellular assays with in vitro HCV cell culture systems identified two ER-localized host proteins RTN1 and RTN3 as novel regulators of HCV propagation. Our analysis builds upon the present understanding of the role of NS5A protein in HCV pathogenesis and provides potential targets for more effective anti-HCV therapeutic intervention.

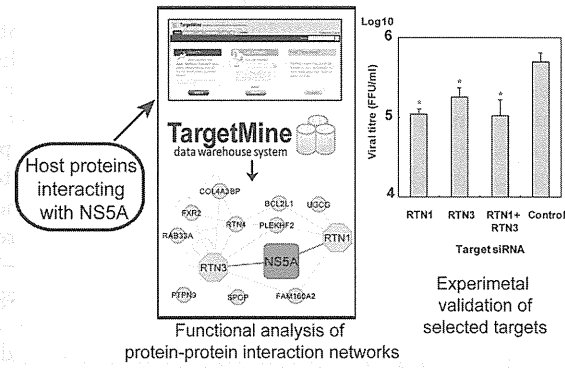

KEYWORDS: *HCV, NS5A, host–pathogen protein–protein interactions, biological network analysis, literature mining, pathway enrichment analysis, siRNA knockdown, target discovery, TargetMine, yeast two-hybrid*

INTRODUCTION

Hepatitis C virus (HCV) causes chronic liver disease including liver steatosis, cirrhosis and hepatocellular carcinoma (HCC) and infects nearly 3% of the world population. HCV possesses a single-stranded RNA genome encoding a 3000 amino acid polyprotein, which is processed by host and viral proteases to yield 10 viral proteins, Core, E1, E2, p7, NS2, NS3, NS4A, NS4B, NS5A and NS5B.[1−5] HCV variants are classified into seven genotypes that display phylogenetic heterogeneity, differences in infectivity and interferon sensitivity.[6,7] However, despite considerable research, a precise understanding of the molecular mechanisms underlying HCV pathology remains elusive.

HCV NS5A protein (hereafter referred to as NS5A) is a RNA binding phosphoprotein, which consists of three domains; domain I includes a zinc-finger motif necessary for HCV replication and an N-terminal membrane anchor region, and the unstructured domains II and III facilitate protein–protein interactions. NS5A plays a critical role in regulating viral replication, production of infectious viral particles, interferon resistance and modulation of apoptosis in HCV pathogenesis via interactions with other HCV proteins and host factors.[8−12] Furthermore, BMS-790052, a small molecule inhibitor of NS5A, is the most potent inhibitor of HCV infection known so far.[13] Consequently, NS5A has emerged as a unique, attractive and promising target for anti-HCV therapy.[14−19] In particular, impairing interactions between NS5A and host factors has been shown to impede HCV infection, which may offer novel anti-HCV therapeutic approaches.[12,20] However, the overall structure and precise functions of NS5A in HCV pathogenesis are poorly understood.

Pathogens such as viruses infect their hosts by interacting with the components of the host cellular networks and

Received: November 30, 2012
Published: May 6, 2013

exploiting the cellular machinery for their survival and propagation. Therefore, elucidating host–pathogen interactions is crucial for a better understanding of pathogenesis.[21−26] Here, we report the host biological processes likely to be influenced by NS5A by virtue of an inferred protein–protein interaction (PPI) network. We describe our integrated approach that combines an experimental yeast two-hybrid (Y2H) assay using NS5A as bait to screen a library of human cDNAs with comprehensive literature mining. The analysis of the NS5A infection network illustrates the functional pathways likely to be influenced by NS5A–host interactions in HCV pathogenesis, thus providing novel insights into the NS5A function in HCV pathogenesis. Furthermore, RTN1 and RTN3, which are endoplasmic reticulum (ER)-localized proteins involved in regulating ER integrity, will be demonstrated as novel regulators of HCV propagation and thus attractive targets for anti-HCV therapy.

MATERIALS AND METHODS

Yeast Two-Hybrid Protein Assay

Screening for the genes encoding host proteins that interact with NS5A was performed using the Matchmaker two-hybrid system (Clontech, Palo Alto, CA, USA) as per the manufacturers' specifications. Human adult liver libraries were purchased from Clontech and were cloned into the pAct2 vector (Clontech) and expressed as fusion proteins fused to the Gal4-activation domain (Gal4-AD). Since Y2H requires the bait protein to translocate to the nucleus, the cDNA of the region corresponding to the NS5A encoding amino acids 1973–2419 (excluding the NS5A N-terminal membrane anchor region) within the HCV polyprotein from the J1 strain (genotype 1b)[27] was amplified by polymerase chain reaction (PCR) and was cloned into the pGBKT7 vector (Clontech)[28] and expressed as Gal4-DNA binding domain (Gal4-DB) fusion in the AH109 yeast strain. The human liver libraries were subsequently screened by Y2H using NS5A as bait. A total of 4×10^6 transformants were screened in this manner, and the positive clones (see Supporting Information) were isolated and sequenced to identify the genes coding for the NS5A interacting host factors (Supporting Information, Table S1).

Literature Mining for Pairwise NS5A–Human Interactions

Literature information describing pairwise interactions between NS5A and cellular proteins were extracted from Medline using the PubMed interface and two other information retrieval and extraction tools, EBIMed[29] and Protein Corral. These tools employ an automatic text-mining approach, but we supplemented them with a follow-up manual inspection. All abstracts related to "NS5A" and "HCV NS5A" keywords and interaction verbs (including "interact", "bind", "attach", "associate")[30] were gathered and manually examined to retrieve direct pairwise NS5A–human protein interactions (see Supporting Information, Tables S2, S3, S4, S5a).

Construction of Extended Protein–Protein Interaction Networks

Physical and direct binary interactions between all human proteins were retrieved from BioGRID 3.1.93[31] and iRefindex 9.0[32] databases using TargetMine.[33] TargetMine is an integrated data warehouse that combines different types of biological data and employs an objective protocol to prioritise candidate genes for further experimental investigation.[33] The interactions were filtered for redundancy, potential false positives and isolated components to infer a representative undirected and singly connected high-confidence human protein interactome (HPI) comprising 22 532 nonredundant binary physical interactions between 7277 proteins (see Supporting Information, Figure S2, Table S5b). The inferred HPI was used to identify biologically relevant trends, the significance of which was assessed by using randomized networks (see below). Secondary interactors of the NS5A interacting proteins were retrieved from the HPI and were appended to the NS5A–host interactions to construct a representative NS5A infection network (Supporting Information, Table S5a).

Topological Analysis

Network components were visualized using Cytoscape,[34,35] while network properties such as *node degree distribution*, *average shortest path* and *betweenness* measures were computed using Cytoscape NetworkAnalyzer plugin[36] as described earlier.[24] For comparison, degree preserved randomized PPI networks were generated by edge rewiring using the Cytoscape RandomNetworks plugin and were used as control networks to assess the statistical significance of the topological trends observed in the inferred PPI networks (see Supporting Information).

Functional Analysis by Characterization of Enriched Biological Associations

Protein structural domain assignments were retrieved from the Gene3D database,[37] Gene ontology associations from the GO consortium,[38] and biological pathway data from KEGG[39] were used to assign functional annotations to the genes in the NS5A infection network. The enrichment of specific biological associations within the NS5A infection network was estimated by performing the hypergeometric test within TargetMine. The inferred p-values were further adjusted for multiple test correction to control the false discovery rate using the Benjamini and Hochberg procedure,[40,41] and the annotations/pathways were considered significant if the adjusted $p \leq 0.005$.

RNAi and Transfection

A mixture of four siRNA targets each to RTN1 and RTN3 (SMARTpool:siGENOME RTN1 siRNA and SMARTpool:siGENOME RTN3 siRNA, respectively) were purchased from Thermo Scientific (Thermo Scientific, Waltham, MA, USA). siGENOME Non-Targeting siRNA Pool #1 (Thermo Scientific) was used as a control siRNA. Thermo Scientific ID numbers of siRNA mixtures of RTN1 and RTN3 and the control were M-014138-00, M-020088-00 and D-001206-13-05, respectively. Each siRNA mixture was introduced into the cell lines by using lipofectamine RNAiMax (Invitrogen, Carlsbad, CA, USA). The replicon cell line, as will be described below, was transfected with each siRNA at a final concentration of 20 nM as per the manufacturer's protocol and then seeded at 2.5×10^4 cells per well of a 24-well plate. The transfected cells were harvested at 72 h post-transfection. The Huh7OK1 cell line, as will be described below, was transfected with each siRNA at a final concentration of 20 nM as per the manufacturer's protocol and then seeded at 2.5×10^4 cells per well of a 24-well plate. The transfected cells were infected with JFH1 at an MOI of 0.05 at 24 h post-transfection. The resulting cells were harvested at the indicated time.

Table 1. List of 132 Human Proteins Interacting with the HCV NS5A Protein

gene ID	symbol	description	refs
47	ACLY	ATP citrate lyase	22
60	ACTB	actin, beta	101
79026	AHNAK	AHNAK nucleoprotein	22
10598	AHSA1	AHA1, activator of heat shock 90 kDa protein ATPase homologue 1 (yeast)	102
207	AKT1	v-akt murine thymoma viral oncogene homologue 1	22
302	ANXA2	annexin A2	103
335	APOA1	apolipoprotein A-I	22
348	APOE	apolipoprotein E	22
116985	ARAP1	ArfGAP with RhoGAP domain, ankyrin repeat and PH domain 1	22
27236	ARFIP1	ADP-ribosylation factor interacting protein 1	22
23204	ARL6IP1	ADP-ribosylation factor-like 6 interacting protein 1	this study
4508	ATP6	ATP synthase F0 subunit 6	this study
8312	AXIN1	axin 1	22
581	BAX	BCL2-associated X protein	22
222389	BEND7	BEN domain containing 7	22
274	BIN1	bridging integrator 1	this study; 22,47
89927	C16orf45	chromosome 16 open reading frame 45	this study
8618	CADPS	Ca^{++}-dependent secretion activator	22
93664	CADPS2	Ca^{++}-dependent secretion activator 2	22
79080	CCDC86	coiled-coil domain containing 86	22
983	CDK1	cyclin-dependent kinase 1	22
1021	CDK6	cyclin-dependent kinase 6	22
1060	CENPC1	centromere protein C 1	22
153241	CEP120	centrosomal protein 120 kDa	22
11190	CEP250	centrosomal protein 250 kDa	22
9702	CEP57	centrosomal protein 57 kDa	22
80254	CEP63	centrosomal protein 63 kDa	22
1381	CRABP1	cellular retinoic acid binding protein 1	22
1445	CSK	c-src tyrosine kinase	22
1452	CSNK1A1	casein kinase 1, alpha 1	104
1457	CSNK2A1	casein kinase 2, alpha 1 polypeptide	63,105
1499	CTNNB1	catenin (cadherin-associated protein), beta 1, 88 kDa	84,106
9093	DNAJA3	DnaJ (Hsp40) homologue, subfamily A, member 3	22
2202	EFEMP1	EGF containing fibulin-like extracellular matrix protein 1	22
5610	EIF2AK2	eukaryotic translation initiation factor 2-alpha kinase 2	22
2051	EPHB6	EPH receptor B6	this study
54942	FAM206A	family with sequence similarity 206, member A	22
25827	FBXL2	F-box and leucine-rich repeat protein 2	22
2274	FHL2	four and a half LIM domains 2	22
23770	FKBP8	FK506 binding protein 8, 38 kDa	this study; 43,45
2316	FLNA	filamin A, alpha	12
2495	FTH1	ferritin, heavy polypeptide 1	22
8880	FUBP1	far upstream element (FUSE) binding protein 1	107
2534	FYN	FYN oncogene related to SRC, FGR, YES	22
11345	GABARAPL2	GABA(A) receptor-associated protein-like 2	this study
54826	GIN1	gypsy retrotransposon integrase 1	22
2801	GOLGA2	golgin A2	22
2874	GPS2	G protein pathway suppressor 2	22
2885	GRB2	growth factor receptor-bound protein 2	22
2931	GSK3A	glycogen synthase kinase 3 alpha	22
2932	GSK3B	glycogen synthase kinase 3 beta	22
3055	HCK	hemopoietic cell kinase	22
3320	HSP90AA1	heat shock protein 90 kDa alpha (cytosolic), class A member 1	22
3303	HSPA1A	heat shock 70 kDa protein 1A	108
3315	HSPB1	heat shock 27 kDa protein 1	109
3537	IGLC1	immunoglobulin lambda constant 1 (Mcg marker)	22
79711	IPO4	importin 4	22
3843	IPO5	importin 5	22
3683	ITGAL	integrin, alpha L (antigen CD11A (p180), lymphocyte function-associated antigen 1; alpha polypeptide)	22
6453	ITSN1	intersectin 1	this study
3716	JAK1	Janus kinase 1	22

Table 1. continued

gene ID	symbol	description	refs
3932	LCK	lymphocyte-specific protein tyrosine kinase	22
55679	LIMS2	LIM and senescent cell antigen-like domains 2	22
4067	LYN	v-yes-1 Yamaguchi sarcoma viral related oncogene homologue	22
9448	MAP4K4	mitogen-activated protein kinase kinase kinase kinase 4	this study
6300	MAPK12	mitogen-activated protein kinase 12	22
4155	MBP	myelin basic protein	22
4256	MGP	matrix Gla protein	110
55233	MOB1A	MOB kinase activator 1A	22
4673	NAP1L1	nucleosome assembly protein 1-like 1	22
4674	NAP1L2	nucleosome assembly protein 1-like 2	22
10397	NDRG1	N-myc downstream regulated 1	22
4778	NFE2	nuclear factor (erythroid-derived 2), 45 kDa	22
11188	NISCH	nischarin	this study
4924	NUCB1	nucleobindin 1	22
4938	OAS1	2′-5′-oligoadenylate synthetase 1, 40/46 kDa	22
5007	OSBP	oxysterol binding protein	111
64098	PARVG	parvin, gamma	22
5170	PDPK1	3-phosphoinositide dependent protein kinase-1	22
5297	PI4KA	phosphatidylinositol 4-kinase, catalytic, alpha	22
5291	PIK3CB	phosphoinositide-3-kinase, catalytic, beta polypeptide	22
5295	PIK3R1	phosphoinositide-3-kinase, regulatory subunit 1 (alpha)	55,84,106
5300	PIN1	peptidylprolyl cis/trans isomerase, NIMA-interacting 1	112
5307	PITX1	paired-like homeodomain 1	22
5347	PLK1	polo-like kinase 1	113
10654	PMVK	phosphomevalonate kinase	22
5478	PPIA	peptidylprolyl isomerase A (cyclophilin A)	114,115
10848	PPP1R13L	protein phosphatase 1, regulatory subunit 13 like	22
5515	PPP2CA	protein phosphatase 2, catalytic subunit, alpha isozyme	116
5518	PPP2R1A	protein phosphatase 2, regulatory subunit A, alpha	116
5698	PSMB9	proteasome (prosome, macropain) subunit, beta type, 9 (large multifunctional peptidase 2)	22
5757	PTMA	prothymosin, alpha	22
5894	RAF1	v-raf-1 murine leukemia viral oncogene homologue 1	22
6142	RPL18A	ribosomal protein L18a	22
6167	RPL37	ribosomal protein L37	this study
6238	RRBP1	ribosome binding protein 1 homologue 180 kDa (dog)	22
91543	RSAD2	radical S-adenosyl methionine domain containing 2	117
6252	RTN1	reticulon 1	this study
10313	RTN3	reticulon 3	this study
6424	SFRP4	secreted frizzled-related protein 4	22
81858	SHARPIN	SHANK-associated RH domain interactor	22
64754	SMYD3	SET and MYND domain containing 3	22
8470	SORBS2	sorbin and SH3 domain containing 2	22
10174	SORBS3	sorbin and SH3 domain containing 3	22
6714	SRC	v-src sarcoma (Schmidt-Ruppin A-2) viral oncogene homologue (avian)	22
10847	SRCAP	Snf2-related CREBBP activator protein	22
6741	SSB	Sjogren syndrome antigen B (autoantigen La)	22
284297	SSC5D	scavenger receptor cysteine rich domain containing (5 domains)	110
6772	STAT1	signal transducer and activator of transcription 1	118
25777	SUN2	Sad1 and UNC84 domain containing 2	this study
6850	SYK	spleen tyrosine kinase	119
4070	TACSTD2	tumor-associated calcium signal transducer 2	22
6880	TAF9	TAF9 RNA polymerase II, TATA box binding protein (TBP)-associated factor, 32 kDa	22
6908	TBP	TATA box binding protein	22
7046	TGFBR1	transforming growth factor, beta receptor 1	22
7057	THBS1	thrombospondin 1	22
374395	TMEM179B	transmembrane protein 179B	22
7110	TMF1	TATA element modulatory factor 1	22
7157	TP53	tumor protein p53	22
7159	TP53BP2	tumor protein p53 binding protein, 2	22
7186	TRAF2	TNF receptor-associated factor 2	22
11078	TRIOBP	TRIO and F-actin binding protein	22